TITLE: Modelling dementia in Drosophila uncovers shared and specific targets of TDP-43 proteinopathy across ALS and FTD relevant circuits

Authors: R Keating Godfrey[1,2], Reed T Bjork[1], Eric Alsop[3], Hillary C Ruvalcaba[1], Jerry Antone[3], Allison F Michael[1], Christi Williams[1], Grace Hala'ufia[1], Alexander D Blythe[1], Megan Hall[3], Kendall Van Keuren-Jensen[3], Daniela C Zarnescu [1,4,*]

AFFILIATIONS:

[1] Department of Molecular and Cellular Biology, 1007 E. Lowell St, Life Sciences South, University of Arizona, Tucson AZ 85721, USA

[2] current address: McGuire Center for Lepidoptera and Biodiversity, Florida Museum of Natural History, 3215 Hull Road, University of Florida, Gainesville, FL 32611, USA

[3] Translational Genomics Research Institute, 445 N 5th St, Phoenix, AZ 85004, USA

[4] current address: Cellular and Molecular Physiology, 500 University Drive Crescent Building C4605, Penn State College of Medicine, Hershey PA 17033, USA

* corresponding author: Daniela C Zarnescu dcz102@psu.edu

ABSTRACT (150-200 words)

Amyotrophic lateral sclerosis (ALS) and fronto-temporal dementia (FTD) comprise a spectrum of neurodegenerative diseases linked to TDP-43 proteinopathy. At the cellular level, TDP-43 proteinopathies are characterized by loss of nuclear TDP-43 and accumulation of cytoplasmic TDP-43 puncta that ultimately cause RNA processing defects including dysregulation of splicing, mRNA transport and translation. Complementing our previous models of ALS, here we report a novel model of FTD based on overexpression of TDP-43 in the Drosophila mushroom body (MB) circuit. This model recapitulates several aspects of FTD pathology including age dependent nuclear depletion and cytoplasmic accumulation of TDP-43 accompanied by behavioral deficits in working memory and sleep that occur before axonal degeneration ensues. RNA immunoprecipitations identify several candidate mRNA targets of TDP-43 in MBs, some of which are specific to the MB circuit and others that are shared with motor neurons. Using genetic interactions we show that overexpression of Dally-like-protein (Dlp), a modulator of Wg/Wnt signaling in MBs mitigates TDP-43 dependent working memory deficits. These results highlight the utility of modelling TDP-43 proteinopathy in Drosophila and provide a novel platform for studying the molecular mechanisms underlying FTD, and potentially uncovering circuit specific vulnerabilities in ALS/FTD.

INTRODUCTION

Characterized by extensive overlap in cellular pathology, genetic mutations, and molecular markers, amyotrophic lateral sclerosis (ALS) and frontotemporal dementia (FTD) comprise a neurodegenerative disease spectrum affecting multiple subsets of neurons in the spinal cord, motor cortex, cingulate cortex, and frontal and temporal lobes (Arai et al., 2006; Ferrari et al., 2011; Ling et al., 2013; Neumann et al., 2006). Notably, nearly 97% of ALS cases (Mackenzie et al., 2007) and approximately 45% of FTD cases (Cairns et al., 2007) exhibit neurodegeneration with ubiquitin-positive cytoplasmic inclusions that contain transactive response (TAR) DNA binding protein 43 (TDP-43). A number of point mutations in *TARDBP*, the gene encoding TDP-43, have been identified as causative of ALS (Kabashi et al., 2008; Rutherford et al., 2008; Sreedharan et al., 2008) while others have been linked to FTD (Borroni et al., 2009; Chen et al., 2019). Although mutations in at least 20 other genes have been associated with ALS/FTD (Al-Chalabi et al., 2012), the majority of ALS/FTD cases are sporadic.

Substantiating its significance as a marker of pathology, TDP-43 has also been identified as a component of cytoplasmic aggregates in dementias other than FTD, including Alzheimer's disease (AD) (Chang et al., 2015; Josephs et al., 2014b; Rohn, 2008), AD with Lewy body dementia (AD/LBD) (McAleese et al., 2017), Parkinsonism-dementia complex (PDC) (Hasegawa et al., 2007), and hippocampal sclerosis (Amador-Ortiz et al., 2007). Up to 57% of AD cases exhibit TDP-43 positive intracellular inclusions (Josephs et al., 2014a); notably, AD patients with TDP-43 proteinopathy show accelerated disease progression with more severe cognitive impairment (Josephs et al., 2014b; Meneses et al., 2021). In addition to the presence of TDP-43 proteinopathy, dementias such as FTD and AD also share TDP-43 associated cellular pathology, including dystrophic neurites (Mackenzie et al., 2011). Thus, despite differences in underlying genetic risk factors and specific neural populations affected, a large proportion of dementias exhibit overlapping TDP-43 pathology, providing a common entry point for understanding shared mechanisms of neurodegeneration (Gao et al., 2018; Jo et al., 2020).

Wild-type TDP-43 is localized primarily to the nucleus where it regulates transcription (Swain et al., 2016) and splicing (Fiesel et al., 2012; Freibaum et al., 2010; Ling et al., 2015; Polymenidou et al., 2011; Tollervey et al., 2011) necessary for nervous system development and function. TDP-43 also shuttles between the nucleus and cytoplasm and has been shown to play a role in axonal and dendritic mRNA localization (Alami et al., 2014; Chou et al., 2018; Fallini et al., 2012), stress granule dynamics (Colombrita et al., 2009; Khalfallah et al., 2018; McDonald et al., 2011) and translation (Altman et al., 2021; Coyne et al., 2017; Lehmkuhl et al., 2021). During severe or prolonged cellular stress and in disease, TDP-43 exits the nucleus and associates with ubiquitin-positive cytoplasmic inclusions (Ramaswami et al., 2013). Indeed, cellular dysfunction and subsequent degeneration associated with TDP-43 pathology have been attributed to both loss-of-function of nuclear TDP-43 (Ling et al., 2015) and cytoplasmic gain-of-function (Walker et al., 2015) whereby cytoplasmic inclusions sequester mRNAs and perturb protein homeostasis (Ramaswami et al., 2013).

Following the identification of TDP-43 as a protein of pathological interest in numerous neurodegenerative diseases, model organisms have been critical to understanding the normal biological functions of TDP-43 and how disruption of these functions leads to disease. Despite having diverged from a common ancestor with vertebrates over 600 million years ago (Erwin, 2015), the fruit fly (*Drosophila melanogaster*) genome contains a homolog of *TARDBP*, namely *TBPH*, which displays sequence similarity and functional overlap with human TDP-43 (Ayala et al., 2005; Estes et al., 2011).

In addition to extensive overlap in neurogenetic homology, circuit-level conservation in the central nervous system has also been demonstrated between invertebrates and vertebrates (Bier, 2005; Bridi et al., 2020; Strausfeld and Hirth, 2013), making invertebrate models relevant for understanding diseases of cognition. Indeed, flies display several behaviors affected in human disease (Muqit and Feany, 2002) including associative learning (Heisenberg, 2003), long-term memory (Isabel et al., 2004), sleep (Shaw et al., 2000), social interactions (Baier et

al., 2002; Kamyshev et al., 2002), and addiction (Bellen, 1998) that can serve as system-level readouts of molecular- and/or cellular-level dysfunction. Models of TDP-43 proteinopathy in *Drosophila* have recapitulated the locomotor phenotypes, motor neuron dysfunction, and shortened lifespan (Estes et al., 2011; Li et al., 2010; Romano et al., 2012) observed in ALS and highlighted degeneration in central brain structures (Li *et al.*, 2010) reminiscent of FTD. Beyond simply simulating disease states, these fly models have identified translational targets (Coyne et al., 2017; Coyne et al., 2014; Lehmkuhl et al., 2021) and genetic modifiers of TDP-43 proteinopathy (Azpurua et al., 2021; Coyne et al., 2015; Sreedharan et al., 2015; Zhan et al., 2013), and exposed systemic effects on metabolic pathways (Loganathan et al., 2022; Manzo et al., 2019).

While TDP-43 proteinopathy has been extensively studied in motor neurons and glia as a model of ALS, a robust fly model of dementia based on TDP-43 proteinopathy has not yet been established. This is in part because the mushroom bodies (MBs) of the fly brain, which were originally described as essential to odor learning (de Belle and Heisenberg, 1994) have only recently been recognized as being required for multi-modal and context-dependent learning (Liu et al., 1999; Vogt et al., 2014) including place learning (Ostrowski et al., 2015). The MBs also regulate sleep (Driscoll et al., 2021; Joiner et al., 2006), satiety (Tsao et al., 2018), social behavior (Sun et al., 2020) and gate behaviors attributed to other brain regions such as decision-making (Zhang et al., 2007) and aggression (Zwarts et al., 2015). Therefore, the MBs share functional overlap with regions of the vertebrate cortex (Wolff and Strausfeld, 2016). Existing fly models of intellectual disability (Mariano et al., 2020) and Alzheimer's disease (AD; (Chakraborty et al., 2011) have either focused on, or identified phenotypes in the MBs of the fly brain, suggesting that this structure is appropriate for modeling diseases of cognition.

Here we describe the development of a novel fly model of FTD based on TDP-43 proteinopathy induced by over-expression of human TDP-43 in a subset of MB neurons. Our model recapitulates key cellular and behavioral characteristics of human dementias with TDP-

43 pathology, including age-dependent loss of nuclear TDP-43, axonal degeneration, and working memory and sleep deficits that parallel those observed in dementia patients. Furthermore, using RNA immunoprecipitations we show that in MBs TDP-43 associates with several mRNAs, a subset of which are specific to MBs while others are shared with mRNA targets previously identified in motor neurons. Interestingly, among the MB candidate targets of TDP-43 we identified *dlp* mRNA, encoding the heparan sulfate proteoglycan (HSPG) Dally-like protein (Dlp)/GPC6, previously shown to be a target of TDP-43 in fly models of ALS and altered in ALS spinal cords (Lehmkuhl *et al.*, 2021). We report that *dlp* mRNA is enriched in TDP-43 complexes in MBs and Dlp protein is decreased within axons in an age-dependent manner, consistent with TDP-43 dependent axonal transport and/or translation deficits. Notably, Dlp overexpression in MBs rescues TDP-43 dependent deficits in working memory consistent with Dlp being a physiologically significant target of TDP-43 in the MB circuit. These findings demonstrate that TDP-43 proteinopathy in MBs causes dementia-like phenotypes that are mediated at least in part by the heparan sulfate proteoglycan (HSPG) Dally-like protein (Dlp)/GPC6, a regulator of the Wg/Wnt signaling pathway. Furthermore, we identify MB specific alterations caused by TDP-43 proteinopathy that may provide insights into neuronal vulnerability across the ALS – FTD spectrum.

RESULTS

Overexpression of TDP-43 in Kenyon cells results in age-dependent nuclear depletion, cytoplasmic mislocalization and cell loss

The insect MBs are comprised of large, complex neurons called Kenyon cells, referred herein as MB neurons (MBNs), which form a layered network with reticular feedback (Crittenden, 1998), structural characteristics reminiscent of vertebrate cortical neurons and networks. There are three subtypes of MBNs based on developmental origin, cell morphology, and wiring. Axons of these three types form five layered lobes, the α/β , α'/β', and γ lobes, which

are further compartmentalized into columnar-like regions based on neuromodulatory inputs and excitatory or inhibitory post synaptic partners (Aso et al., 2014). To model FTD-like TDP-43 proteinopathy we used a split GAL4 driver line SS01276 available from the Janelia FlyLight Split-GAL4 Driver Collection (Aso, 2021) to express human TDP-43 (Estes et al., 2013) in a subset of MBNs that contribute to α/β and γ lobes of the *Drosophila* mushroom bodies. Neurons forming the γ lobes are embryonic in origin and persist through metamorphosis, whereas those comprising the α/β lobes are born during the larval stage (Kunz et al., 2012). Using the SS01276 driver we found TDP-43 to be expressed in approximately 50 larval MBNs in both *TDP-43*^{WT} and mutant expressing brains (Figure 1A,1F *TDP-43*^{WT}; Figure 1-supplement 1, *TDP-43*^{G298S}, P = 0.309). Visual inspection indicated that TDP-43 was largely confined to the nucleus at this juvenile age (Figure 1A) but became mislocalized outside the nucleus in young adults. The nucleus comprises nearly all of the cell body in MBNs, making it challenging to accurately assess cytoplasmic mislocalization or nuclear depletion. Therefore, to determine age-dependent changes in TDP-43 localization, we measured signal intensity of TDP-43 YFP in the nucleus, then measured total TDP-43 in the cell body by tracing the YFP signal around the cell boundary (see Materials and Methods), with the resulting ratio reflecting nucleus to total cell signal intensity (Figure 1D, E). This ratio should be close to 1 when TDP-43 is contained largely in the nucleus or when TDP-43 is localized to the nucleus and the cytoplasm (because the cytoplasm constitutes only a small fraction of the total cell body area). However, when TDP-43 is depleted from the nucleus, this ratio will be smaller than 1. Using this measure of nuclear depletion, we found a significant decrease in the mean signal intensity ratio across the population of MBNs from juvenile to young adults in the context of both TDP-43 variants (Figure 1E, *TDP-43*^{WT} larval, 0.978$\pm$0.005 vs. young adult, 0.869$\pm$0.009, P < 0.0001; Figure 1-supplement 1, *TDP-43*^{G298S} larval, 0.967$\pm$0.002 vs young adult, 0.906$\pm$0.012, P = 0.0004; supplemental table S1E). Surprisingly, this ratio increased in old adult brains compared to young adults, however, it was

still significantly lower than at the juvenile age time point in our *TDP-43^{WT}* model (Figure 1E, larval vs. old adult, 0.927±0.009, P = 0.0041; supplemental table S1E). A plausible explanation for this result is provided by our findings that there are significantly fewer YFP positive MBNs in old TDP-43 brains than in younger TDP-43 brains or in old YFP controls (*TDP-43^{WT}* old adult [445±96 cells] vs young adult, 1089±40 cells or vs. YFP old adult, 1206±150 cells, P < 0.001; Figure 1F; *TDP-43^{G298S}* old adult, 473±79 cells vs young adult, 1097±55 cells and vs YFP old adult, 1206±150 cells, P < 0.001; Figure1-supplement 1; supplemental table S1F) consistent with TDP-43 overexpression causing cell loss with age. This also suggests that the MBNs with increased cytoplasmic TDP-43 are more vulnerable and more likely to undergo cell death during aging.

Mushroom body axons exhibit age-dependent TDP-43 aggregation and progressive degeneration

To determine the effect of TDP-43 proteinopathy on axonal integrity, we co-expressed TDP-43 and the membrane marker mCD8 RFP. Signal intensity of mCD8 RFP showed progressive loss in the γ lobe over time (young, 1.01±0.04, middle-aged, 0.87±0.25, and old, 0.40±0.10 fluorescence intensity ratio to controls; Figure 2A, B, insets b, e, h; quantified in C; supplemental table S2A), suggesting that axonal degradation occurred in an age-dependent manner. Simultaneously, *TDP-43 YFP* formed increasingly larger axonal aggregates in the γ lobe with age (young, 1.00±0.04, middle-aged, 1.19±0.05, and old, 1.35±0.05 area normalized to controls Figure 2B, insets c, f, i; quantified in D; supplemental table S2B). A similar pattern of axonal fragmentation in the γ lobe, coincident with increased TDP-43 aggregation size, was observed in flies over-expressing *TDP-43^{G298S}* (Figure 2-supplement 1A, B insets c, f, i, quantified in C and D; supplemental tables S2A, S2B). We could not detect statistically significant changes in mCD8 RFP signal intensity nor TDP-43 YFP aggregation size in the α/β

lobes of *TDP-43*^{WT}, however these lobes showed dramatic, age-dependent thinning not observed in controls (Figure 2B inset i). In *TDP-43*^{G298S} expressing brains, we observed both an increase in the size of TDP-43 aggregates within α/β lobes between young and middle-aged adults, and a thinning of these lobes (Figure 2-supplement 1B inset i). These phenotypes are reminiscent of the age-dependent pathophysiology observed in human patients. Given that γ lobe neurons are born earlier than those within the α/β lobes, the more severe phenotypes observed in this neuronal subpopulation highlight the aging component of TDP-43 proteinopathy.

TDP-43 proteinopathy causes working memory deficits

In humans, working memory is disrupted in FTD and other TDP-43 associated dementias (Poos et al., 2018; Stopford et al., 2012). To test whether flies overexpressing TDP-43 exhibit working memory deficits, we used miniature Y-mazes to measure spontaneous alternation behavior by scoring three consecutive arm entries over a period of ten minutes (see Materials and Methods, Figure 3A, Lewis et al., 2017). These experiments showed that although TDP-43 overexpression results in increased overall movement (males: *TDP-43*^{WT}, 146.00$\pm$7.51 mm vs. OR-R control, 106.19$\pm$8.18 mm, P = 0.018; females: *TDP-43*^{WT,} 110.53$\pm$7.51 mm vs. OR-R control, 81.12$\pm$5.24 mm; Figure 3B; for means of individual replicates see supplemental table S3), percent alternation is significantly decreased in young adult males (*TDP-43*^{WT}, 0.57$\pm$0.01 vs. OR-R control, 0.61$\pm$0.01, P = 0.012) and females (*TDP-43*^{WT}, 0.60$\pm$0.02 vs. OR-R control, 0.65$\pm$0.01, P = 0.006; Figure 3C), consistent with working memory deficits.

TDP-43 expression in the MB circuit causes sleep alterations

Frontal and temporal lobe degeneration is associated with increased daytime somnolence (Sani et al., 2019). Overall, sleep disturbances are highly variable in FTD and may

be detectable in earlier stages than in AD (Bonakis et al., 2014). To determine whether TDP-43 proteinopathy in the MB circuit alters sleep, we used Drosophila Activity Monitors (DAMs, see Materials and Methods) to measure total daytime and nighttime sleep. Our experiments show that on average, both male and female TDP-43 expressing flies appear to be lethargic; they spent a greater proportion of their time sleeping during both the day and night compared to controls (approximately 11% more for *TDP-43*^{WT} and approximately 8% more for *TDP-43*^{G298S}). However, there are subtle differences in how TDP-43 OE affects sleep patterns based on age and sex. While males consistently sleep more during the day, this effect is weaker in females flies where we found trends towards increased daytime sleep at some but not all age time points in each genotype (Figure 4A; supplemental table S4A). At night, males and females also exhibited a general tendency towards increased sleep with the exception of young TDP-43 expressing adult males which, when compared to w^{1118} controls, showed signs of sleep fragmentation as evidenced by more frequent, shorter sleep bouts (Figures 4B, C for *TDP-43*^{WT} and Figure 4-supplement 1B, C for *TDP-43*^{G298S}*;* supplemental table S4B,C).

Interestingly, both humans and flies show decreased nighttime sleep with age (Li et al., 2018); in line with this, w^{1118} flies of both sexes showed age-related declines in nighttime sleep, whereas TDP-43 males showed no such declines (all pairwise comparisons $P > 0.05$) and female declines appear less steep (*TDP-43*^{WT}, Figure 4B; *TDP-43*^{G298S}, Figure 4-supplement 1; supplemental tables S4A), consistent with our findings that TDP-43 proteinopathy causes lethargy. By middle age, *TDP-43*^{WT} males showed a pattern of longer, less frequent nighttime sleep bouts as compared with w^{1118} (Figure 4C). Within each genotype, female w^{1118} and *TDP-43*^{WT} flies exhibited age-related sleep fragmentation as evidenced by a greater number of shorter bouts at 60 - 63 days compared with 1 – 3 days. TDP-43 flies still spent a greater proportion of their time sleeping than controls (Figure 4B; supplemental table S4A), an effect driven by longer sleep bouts at this aged time point (Figure 4C; supplemental table S4B). Taken together, these results indicate that TDP-43 expression in the MB circuit causes sleep deficits

resembling those reported in FTD patients, including increased sleep during the day and sleep fragmentation at night, albeit the latter was detected in young males only. Notably, the sleep fragmentation phenotype occurs concomitant with the nuclear depletion of TDP-43 and before axonal degeneration suggesting that this is a direct consequence of TDP-43 mislocalization while lethargy may an indirect consequence of large-scale neuronal degeneration.

TDP-43 overexpression in Kenyon cells is sufficient to reduce lifespan in Drosophila

Life expectancy for FTD patients after diagnosis is approximately 8 – 12 years and while patients do not often die from the disease itself, there is a measurable, if subtle, effect on life expectancy (Kansal et al., 2016; Loi et al., 2021). We therefore tested whether TDP-43 proteinopathy affects lifespan in our fly model and found that overexpression of TDP-43 in MBNs significantly reduces median survival time for *TDP-43*^{WT} (84 days, 95% CI [84,84]) and *TDP-43*^{G298S} (89 days, 95% CI [88,91]) when compared with YFP controls (94 days, 95% CI [90, 95]; $P < 0.0001$ and $P = 0.028$, respectively; Figure 5 and Figure 5-supplement 1). These results indicate that overexpression of TDP-43 in a subset of MBNs is sufficient to produce a nearly 10% reduction in median lifespan.

mRNAs enriched with TDP-43 in mushroom body neurons exhibit overlap with motor neuron specific candidate targets including components of the Wnt/Wg signaling pathway

To understand how TDP-43 overexpression influences the MBN proteome and whether our model recovers previously identified TDP-43 target mRNAs and genes dysregulated in human FTD, we immunoprecipitated YFP-tagged *TDP-43*^{WT} or *TDP-43*^{G298S} from Drosophila heads expressing TDP-43 in MBNs using the SS01276 GAL4 driver. Next, we used DESeq2 (Love et al., 2014) to assess differential expression of mRNAs enriched in TDP-43 complexes with the whole brain transcriptome. We chose to identify TDP-43 enriched candidate mRNA targets using young adult flies (1 – 3 days post-eclosion), before age-dependent axonal

neurodegeneration is detected in the MB lobes, to avoid detection of gene expression alterations that could be an indirect consequence of neurodegeneration. Of the 13,302 transcripts detected in the fly brain, we identified 1055 and 1393 candidate mRNA targets based on their enrichment in *TDP-43*^{WT} and *TDP-43*^{G298S} complexes, respectively (Log2FC > 1 compared to the brain transcriptome, Padj < 0.05) (Figure 6A, Figure 6-supplement 1A). A total of 876 candidate mRNAs were shared by both variants (83% of targets in *TDP-43*^{WT} and 63% of targets in *TDP-43*^{G298S}), for a total of 1572 mRNAs enriched across both models (with 179 unique to *TDP-43*^{WT} and 517 to *TDP-43*^{G298S}, respectively). Notably, differential expression analyses also recovered previously identified TDP-43 target mRNAs including *futsch* (*TDP-43*^{WT} Log2FC = 1.81, P_{adj} = 2.66E-07; *TDP-43*^{G298S} Log2FC = 2.14, P_{adj} = 9.57E-10) (Coyne *et al.*, 2014) and *dscam2* (*TDP-43*^{WT} Log2FC = 1.29, P_{adj} = 6.01E-04; *TDP-43*^{G298S} Log2FC = 1.81, P_{adj} = 2.42E-3) (Xiao et al., 2011).

While TDP-43 has been found to interact with mRNA in a cell type specific manner, there is also overlap in TDP-43 associated targets within the central brain and in motor neurons under both physiological and pathological conditions (Susnjar et al., 2022). In line with this, we found that nearly 44% of *TDP-43*^{WT} and 42% of *TDP-43*^{G298S} highly associated MBN mRNAs overlapped with those we identified previously when modeling ALS by overexpressing TDP-43 in motor neurons with the D42 GAL4 driver (Figure 6B, Figure 6-figure supplement 1C). Additionally, among the mRNAs enriched with TDP-43 in flies we identified several orthologs of human genes enriched in the frontal cortices of FTD patients including the Ras family member RHOQ (*Rac2*, *TDP-43*^{WT} Log2FC = 3.68, Padj = 9.66E-24), the glypican GPC4 (*dlp*, *TDP-43*^{WT} Log2FC =3.33, Padj = 9.14E-23), heat shock 70kDa protein 2, HSPA2 (*Hsp70Bb*, *TDP-43*^{WT} Log2FC = 2.77, Padj = 1.59E-7), and the frizzled family receptor protein FZD7 (*fz*, *TDP-43*^{WT} Log2FC = 2.18. Padj = 4.25E-12) (Santiago et al., 2020).

Functional annotation of targets enriched in the MBs identified neuron-specific as well as neuromuscular junction molecular pathways in both the *TDP-43*^{WT} and *TDP-43*^{G298S} models

(Figure 6-supplement 2A). Interestingly, components of the Wingless (Wg/Wnt) signaling pathway were overrepresented in the TDP-43 proteinopathy model of FTD (Figure 6-supplement 2B). Highly enriched members of these pathways include frizzled (*fz*), a Wg/Wnt receptor, dally-like protein (*dlp*), a heparan sulfate proteoglycan (HSPG) that interacts with multiple Wnt ligands (Waghmare et al., 2020), and the Wg/Wnt receptor Frizzled 2 (Yan et al., 2009). Interestingly, *dlp* mRNA was also found to be enriched with TDP-43 in fly motor neurons, where TDP-43 proteinopathy causes the accumulation of Dlp puncta in cell bodies and simultaneous depletion of Dlp from the neuromuscular junction (Lehmkuhl et al., 2021). To validate that *dlp* mRNA is a target of TDP-43 in MBNs as predicted by RNA seq, we used RNA IPs followed by RT-qPCR and confirmed that *dlp* mRNA is enriched in immunoprecipitated *TDP-43*^{WT} and *TDP-43*^{G298S} complexes compared to input (Figure 6-supplement 1). Taken together, these results show that some mRNAs enriched with TDP-43 in the MB circuit are specific to MBNs while others are shared with MNs and suggest that the Wg/Wnt signaling pathway may be a functional target of TDP-43 proteinopathy in FTD.

TDP-43 proteinopathy causes severe age-related loss of Dally-like protein in MBNs

Given *dlp* mRNA's enrichment with TDP-43, we hypothesized that Dlp protein expression may be affected in MBNs, as we previously found in motor neurons (Lehmkuhl et al., 2021). While Dlp has been shown to be highly expressed in developing MBN axons, where it is thought to be involved in axon guidance (Rawson et al., 2005), its expression and function in adult MBNs is unknown. We found that, despite *dlp* mRNA being enriched in TDP-43 complexes in young adult brains, the levels and distribution of Dlp protein in TDP-43 expressing flies are comparable with controls at that age (Figure 7C, D). Interestingly, Dlp levels decline with age in both controls and TDP-43 OE flies, however while Dlp is still visible in control fly brains at 50 days, Dlp is nearly undetectable in the brains of flies OE TDP-43 (Figure 7A; quantified in B, $P < 0.05$). These findings are consistent with *dlp* mRNA being a target of TDP-43 in MBNs and suggest

mRNA localization and/or translation as possible mechanisms for the observed reduction in Dlp protein expression.

Dlp over expression rescues TDP-43 dependent working memory deficits

We next wanted to evaluate the physiological significance of *dlp* mRNA as a target of TDP-43 in MBs. To address this, we tested whether overexpression of *dlp* mRNA (dlp^{OE}) in the context of TDP-43 proteinopathy could mitigate TDP-43 dependent working memory deficits. Using the Y-maze working memory assays we found that the percent alternation deficits displayed by $TDP\text{-}43^{WT}$ flies could indeed be mitigated by dlp^{OE} in MBNs (Figure 7G). To account for altered movement caused by TDP-43 proteinopathy ($TDP\text{-}43^{WT}$, 147.52 $\pm$ 13.52 mm, w^{1118}, 229.89 $\pm$ 7.43 mm, $P < 0.0001$), we also compared distance-scaled alternations across genotypes and found that TDP-43 dependent alternation deficits were still mitigated by dlp^{OE} ($TDP\text{-}43^{WT}$, 0.0221 $\pm$ 0.0028 alternation/mm, $TDP\text{-}43^{WT}dlp^{OE}$, 0.0286 $\pm$ 0.0036 alternation/mm, $P < 0.0001$; dlp^{OE}, 0.0252 $\pm$ 0.0032 alternation/mm, $TDP\text{-}43^{WT}dlp^{OE}$, $P > 0.05$). We note that although total movement in the Y-maze assay is influenced by the genetic background (w^{1118} versus OR-R, compare Figures 3B and 7C), the alternation phenotype is consistently significantly reduced in TDP-43 OE flies (Figures 3C and 7D). These experiments indicate that Dlp overexpression in the MB circuit mitigates $TDP\text{-}43^{WT}$ dependent working memory deficits as evidenced by the rescue of alternation behavior in the Y-maze assay. Taken together, these findings support the notion that *dlp* mRNA is a functional target of TDP-43 *in vivo* and mediates, at least in part, TDP-43 dependent FTD phenotypes in *Drosophila*.

DISCUSSION

Neurodegenerative diseases have historically been classified by shared symptomology and post-mortem pathology. More recently, the integration of molecular markers and genetic testing has uncovered evidence that cell-type susceptibility and dysregulation of specific

molecular pathways can interact to produce similar clinical presentations across different disease etiologies (Pennington et al., 2011). These findings highlight convergent pathomechanisms during the degeneration process (Gao et al., 2018; Ling et al., 2013) and suggest inroads for better understanding of these complex diseases.

A common pathological feature of several neurodegenerative diseases including ALS, FTD and other dementias is the nuclear depletion of the RNA binding protein TDP-43 accompanied by the accumulation of cytoplasmic, ubiquitinated foci (Mackenzie et al., 2010) (Amador-Ortiz et al., 2007; Chang et al., 2015; Josephs et al., 2014b; McAleese et al., 2017; Rohn, 2008). Since these dementias are often confirmed post-mortem by the presence of TDP-43 pathology, animal models play an important role in elucidating the molecular mechanisms underlying TDP-43 proteinopathy and its role in neurodegeneration. Among these, fly models have proven their utility in this research landscape in part because the availability of powerful molecular and genetic tools allowing multiple hypotheses to be pursued in parallel on a large scale. Indeed, fly models of TDP-43 proteinopathy based on loss of function or overexpression in the entire nervous system (Feiguin et al., 2009; Lu et al., 2009; Romano et al., 2012), or in subsets of neurons including associative regions of the central brain (Li et al., 2010), motoneurons (Estes et al., 2011) or the retina (Elden et al., 2010) have revealed a broad repertoire of altered pathways that have subsequently been confirmed in patient tissues (Coyne et al., 2017; Coyne et al., 2014; Lehmkuhl et al., 2021).

It has been previously shown that overexpression of TDP-43 in all MBNs using the driver line OK107 GAL4 (RRID:BDSC_854) caused age-dependent cell loss and axonal degeneration in MBs, however degeneration severity varied widely across nearly isogenic individuals, challenging its utility as a disease model (Li et al., 2010). This variability could be in part attributed to driver line “leakiness” as OK107 GAL4 drives expression beyond MBs, in optic lobe neuropils (Aso et al., 2009; Morante and Desplan, 2008) and neurosecretory cells (Enell et al., 2010; Hampel et al., 2011).To develop a robust and MB specific model of TDP-43 driven

dementia in *Drosophila melanogaster,* we leveraged a split GAL4 driver line with limited expression to a subset of Kenyon cells (γ, α/β MBNs). Notably, this model exhibits nuclear depletion and cytoplasmic accumulation of TDP-43, accompanied by age-dependent axonal degeneration and cell loss, recapitulating key aspects of disease pathology. Importantly, the onset of FTD relevant behavioral symptoms is detectable prior to widespread degeneration, as observed in human disease. Additionally, this model identifies mRNA targets that have previously been associated with TDP-43 pathology and shows that depletion of one of those targets, *dlp*, mediates, at least in part, TDP-43 dependent working memory deficits in the fly model.

Neurodegeneration in ALS/FTD is thought to be driven by both loss of nuclear function, as some nuclei become devoid of TDP-43, and cytoplasmic gain of toxic function, as evidenced by TDP-43 accumulation in cytoplasmic puncta. While thus far invertebrate models of TDP-43 proteinopathy have not faithfully recapitulated TDP-43 mislocalization (*e.g.*, Ash et al., 2010; Estes et al., 2013), here we found that TDP-43 over-expression in MBNs more closely resembles disease pathology. Indeed, TDP-43 displays normal localization in the juvenile stage but becomes depleted from the nucleus and mislocalized to the cytoplasm in young adults. Axonal degeneration is evident only in older adult flies and differentially affects MBNs that form the α/β and γ lobes, with the latter showing the greatest degeneration severity. This is particularly interesting because MBNs that form the γ lobe are embryonic in origin and therefore older than the pupal-born MBNs that form the α/β lobes (Ito et al., 1997; Kunz et al., 2012; Yu and Lee, 2007), highlighting the aging component of neurodegeneration. It is also possible that the differences in the onset and effects of TDP-43 proteinopathy we observed in γ lobe MBNs may be due to their remodeling during metamorphosis (Kunz et al., 2012), which may increase their vulnerability to TDP-43. Taken together, these findings parallel differential susceptibility observed in human cortical neurons (Nana et al., 2019; Seeley, 2008). Given the availability of

split GAL4 driver lines for subsets of MBNs (Aso et al., 2014) future studies could focus on better understanding of what drives this susceptibility by modeling TDP-43 proteinopathy in various neuronal subpopulations within the MB circuit. It will be interesting to combine these powerful genetic tools with single cell RNA seq efforts in patients and flies in order to pinpoint specific cell sub-types that may be more vulnerable.

Frontotemporal lobar degeneration with TDP-43 proteinopathy (FTLD-TDP) is pathologically classified based on the cortical layers affected, the number of dystrophic neurite, and the extent of neuronal cytoplasmic inclusions (Mackenzie et al., 2011). This pathology is also commonly observed in Alzheimer's disease and dementia with Lewy bodies cases that exhibit TDP-43 proteinopathy, although different brain regions are selectively affected (Josephs et al., 2014a; Josephs et al., 2014b). Interestingly, we find that neuronal cytoplasmic inclusions are absent in juveniles, appear first in young adult brains and increase in size during aging. This neuropathology precedes observations of dystrophic neurites, which are first visible around middle age, increase in severity during aging, and ultimately degenerate. This age-dependent pathology observed in the fly brain parallels that observed in human disease and provides a platform for studying the progression of neurodegeneration in this genetically tractable model.

In humans, behavioral symptoms of FTD precede widespread degeneration by years suggesting that behavioral deficits arise prior to widespread degeneration and without complete loss of TDP-43 function or cytoplasmic aggregation (Perry et al., 2017). Therefore, we chose to focus primarily on working memory and sleep deficits using young adult flies, in which a subset of MBNs show nuclear depletion accompanied by widespread TDP-43 mislocalization to the axonal cytoplasm while MBN axons still appear largely intact. At this young age, we found both working memory and sleep fragmentation phenotypes, albeit the latter were only significant in males. We also assessed these behaviors in aged flies, however the distinct age-dependent deficits exhibited by the controls themselves confounded the detection of TDP-43 specific phenotypes.

Behavioral variant frontotemporal dementia (bvFTD) is diagnosed based on often subtle behavioral symptoms including a lack of empathy, increased apathy and compulsive behaviors, and deficits in executive function (Rascovsky et al., 2011). FTD was classically distinguished from AD using a perceived lack of memory deficits, however recent patient studies and meta-analyses indicate that memory deficits are common in bvFTD and at times indistinguishable between AD and bvFTD (Graham et al., 2005; Pennington et al., 2011), challenging the validity of the exclusion of episodic memory deficits in the clinical diagnoses of bvFTD (Hornberger and Piguet, 2012). Although sleep symptoms are notoriously variable and understudied across different FTD diagnoses, the most common sleep disturbances observed in bvFTD patients are sleep fragmentation and daytime sleepiness that may or may not be accompanied by insomnia (Bonakis et al., 2014; McCarter et al., 2016; Sani et al., 2019). Our findings of limited sleep fragmentation and daytime sleepiness highlight potential differences between the fly model and human disease presentation. That said, the limited yet specific deficits caused by TDP-43 OE in MBNs provide a robust measurable sleep disruption that can serve as an organism-level output for future molecular or pharmacological intervention experiments.

In addition to observed behavioral deficits, flies with TDP-43 proteinopathy show an approximately 10% reduction in median lifespan. This may be roughly comparable to human patients where FTD exerts a subtle effect on lifespan. In humans, mean age at diagnosis is 61.9 for early onset disease (< 65 years) with mean survival after diagnosis around 8 years (Kansal et al., 2016), meaning survival is reduced in comparison with the general population in most countries were clinical data are collected (*e.g.*, 78.8 years in the United States Murphy et al., 2021). Effects on lifespan may be far more severe than a simple comparison of life expectancy would indicate, as Loi et al. (2021) report an increase in mortality risk for FTD patients when compared with age-matched controls. From the perspective of a fly model, it is somewhat surprising to see a lifespan effect given that MBNs comprise a small fraction of total neurons in the fly brain and are often thought to be largely dispensable for viability (de Belle and

Heisenberg, 1994). There is evidence that lifespan is regulated at least in part by the α/β MBNs (Lien et al., 2020), a subset of MBNs included in our model, however loss of key MB proteins such as DCO (Yamazaki et al., 2007) or over-expression of vertebrate TAU in MBNs result in severe memory deficits without affecting lifespan (Mershin et al., 2004). Thus, our model provides additional evidence that specific populations of MBNs may play a role in lifespan regulation in flies, while reproducing an important, subtle characteristic of FTD.

Sequestration of mRNAs is one the mechanisms by which TDP-43 is thought to contribute to neurodegeneration and identifying candidate mRNA targets has helped better understand disease etiology (Bjork et al., 2022; Ramaswami et al., 2013). Although our model is based on TDP-43 overexpression, we note that among the mRNAs enriched with TDP-43 in MBNs we found 12 of 15 physiological targets of TDP-43 previously identified bioinformatically as potential targets of Drosophila TDP-43 (*i.e.*, TBPH) based on UG-richness (Langellotti et al., 2018). In future studies, it will be interesting to explore the relationship between splicing and translational targets of TDP-43. Furthermore, the overlap and specificity of some targets for MNs versus MBNs may provide insights into shared mechanisms and neuronal vulnerability in ALS and FTD, respectively.

Functional analyses of the mRNAs associated with TDP-43 identify numerous cellular pathways including Wg and Hippo that have been previously implicated in sleep regulation in flies (Harbison et al., 2017). Additionally, our findings of dopamine receptors as candidate mRNA targets is consistent with findings that loss of mesocortical dopaminergic tracts and dopamine receptors in the frontal lobes could contribute to the behavioral symptoms in FTLD (Murley and Rowe, 2018).

For functional validation we chose to focus on *dlp*, an mRNA target of TDP-43 that we previously identified in the ALS model of TDP-43 proteinopathy, and a known regulator of Wg signaling. Indeed, Wg signaling is dysregulated in ALS (Chen et al., 2013; Gonzalez-Fernandez et al., 2019), and mRNAs associated with Wg/Wnt pathway are enriched in FTD patient frontal

cortices (Santiago et al., 2020), however, this pathway has not yet been broadly implicated in FTD pathophysiology. Using genetic interactions, we found that *dlp* OE in MBNs mitigates TDP-43 dependent working memory deficits, as evidenced by improved alternation in the Y maze assay. Taken together, these findings support the notion that Wg/Wnt signaling is altered in ALS/FTD and modulating its activity via Dlp mitigates behavioral deficits caused by TDP-43 proteinopathy. In future studies it will be interesting to see how different mRNA targets mitigate specific phenotypic aspects of FTD and identify ALS versus FTD specific targets of TDP-43 proteinopathies.

MATERIALS AND METHODS

Drosophila genetics and maintenance

Specific information on Drosophila lines used in this study can be found in the Key Resources table (Supplementary information). Cytoplasmic YFP was used as a control in experiments with overexpression of YFP-tagged TDP-43. Flies were maintained at 25°C in 12-hour light-dark cycle with 25-30% humidity. To age flies, newly eclosed virgin male and female flies were collected and maintained on standard fly cornmeal/molasses media refreshed weekly until flies were used in experiments. For TDP-43 localization and cell loss experiments, 1 - 3, 30 - 35, and 50 - 55 day old flies were classified as young, middle-aged, and old adults, respectively. For MB lobe anatomy and behavioral assays, we used slightly older flies (60 - 65 days) for the old adult category. Flies harboring UAS TDP-43 YFP and UAS dlp transgenes for co-overexpression of TDP-43 and Dlp were generated using standard genetic recombination techniques. We confirmed that Dlp is indeed overexpressed in the fly nervous system as compared with w^{1118} controls using the pan-neuronal driver, elav GAL4. Expression levels of Dlp were validated using RT-qPCR (dlp^{OE} = 2.45 FC, $TDP\text{-}43^{WT}$;dlp^{OE} = 3.09 FC, $TDP\text{-}43^{G298S}$;dlp^{OE} = 1.71 FC; Figure 6-supplement 1B) and show that Dlp overexpression is likely higher in $TDP\text{-}43^{WT}$ model (Figure 7-supplement 1).

Statistical analyses

Statistical analyses were conducted in R (v. 4.1.2, R CoreTeam, 2021) and Rstudio (v. 2021.09.0+351, RStudioTeam, 2022) unless specified otherwise in specific methods. The tidyverse (Wickham et al., 2019) and ggpubr (Kassambara, 2020) packages were used for summary statistics and graphics. Other analysis-specific packages are cited in the corresponding Methods section. While data for the mutant *TDP-43*^{G298S} model is presented as a supplement to our main findings, statistical analyses were conducted simultaneously for both TDP-43 genotypes and p-values were corrected for multiple comparisons that included both genotypes. For any given analysis when males and females did not differ statistically or sample sizes were low (*e.g.*, histological preparations), they were pooled to increase power. Where necessary, outliers were removed prior to hypothesis testing. When data did not fit the assumptions of parametric models and non-parametric analyses were used, hypothesis testing proceeded by first using a Kruskal-Wallace to test for a difference among groups, followed by pairwise comparisons using the Wilcoxon Rank Sum Test with p-values adjusted for multiple comparisons using the false discovery rate method (Benjamini and Hochberg, 1995). Specific statistical methods used in each assay described below. Summary statistics for each figure can be found in the Supplemental tables and Source Data files are available from ScholarSphere (doi:10.26207/jq6p-w169).

Mushroom body morphological analyses

Immunofluorescence: Mushroom body morphology was evaluated using membrane-targeted RFP (mCD8 RFP) driven by SS01276 (Aso, 2021). Adult brains were dissected in cold HL-3 saline (Stewart et al., 1994), fixed for 60 minutes in 4% paraformaldehyde, then rinsed in phosphate buffered saline (PBS, 3X), permeabilized in 0.25% Triton X-100, and blocked in PBST plus 5% normal goat serum (Sigma-Aldrich 566380) 2% bovine serum albumin (Sigma-

Aldrich A5611) for 45 minutes prior to antibody labeling. YFP was detected by incubating brains overnight at 4°C with a mouse monoclonal anti-GFP FITC antibody (1:300, Rockland 600-302-215). mCD8 RFP was visualized using native fluorescence. All brains were mounted on slides with the ventral side containing the mushroom body lobes (MBLs) facing the coverslip. For cell body imaging, brains were additionally incubated in Hoechst (1:10,000 Invitrogen H3570) for 10 minutes and mounted on slides with the dorsal side containing the calyx facing the coverslip.

Image acquisition and analysis

TDP-43 cytoplasmic localization and MBN cell loss: Images were acquired using a Zeiss 880 Laser Scanning Confocal inverted microscope with a Plan-Apochromat 63x/1.4 oil DIC M27 lens. TDP-43 YFP signal intensity was quantified per unit area in the nucleus and cell body. Hoechst was used to define the nuclear boundaries, while total cellular TDP-43 signal was measured by tracing a boundary around YFP signal in the entire cell. To quantify the total number of MBNs expressing hTDP-43, all nuclei were counted from optical sections 2 μm apart to ensure nuclei were counted only once. We tested for differences in TDP-43 nuclear to cellular ratio and MBN number by age, sex, and genotype using Analysis of Variance (ANOVA) performed on a linear model (*lm* function in R; R Core Team 2017). Residuals were normally distributed (Shapiro-Wilks test for normality, $P = 0.890$ and $P = 0.395$ for ratio and MBN number, respectively) and we therefore continued with pairwise comparisons using Tukey's Honest Significant Difference corrected for multiple comparisons.

Signal intensity: All images were acquired using a Zeiss 880 Laser Scanning Confocal inverted microscope with a Plan-Apochromat 63x/1.4 oil DIC M27 lens. For mCD8 RFP fluorescence intensity, brains were imaged using either an Alexa Fluor 568 or a DS Red filter set with pinhole adjusted to 1 AU and 3 μm optical section thickness. For measuring anti-GFP FITC fluorescence intensity, brains were imaged using the FITC filter set with the pinhole

adjusted to 1 AU and 0.5 μm optical section thickness. Fluorescence intensity was measured as the integrated density over the sample area in axons by manually tracing α/β or γ lobes and subtracting adjacent background signal. First, a polygon was traced free-hand over the visible area of each lobe (α/β or γ). This polygon was then dragged to an adjacent area of the brain to obtain a mean fluorescence intensity for the background in each section. In instances where the polygon was shaped in such a way that it could not be dragged to adjacent brain area, a comparably-sized polygon was drawn in the adjacent brain region. Intensity was measured in at least three sections to obtain mean fluorescence intensity in each channel (RFP or FITC) for both α/β and γ lobes of each brain. To test for differences in signal intensity within a genotype across age time points, values of signal intensity were normalized to mean signal intensity of young (1- 3 day old) brains of the same genotype and lobe. Statistical analysis of change in fluorescence intensity with age was performed by comparing middle aged (~30 days) or old (~60 days) flies and young (~1 day) flies from the same genotype using the Wilcoxon Rank Sum test. Summary statistics can be found in Supplemental table S2A.

YFP particle size: The Analyze Particles function in FIJI was used to identify YFP puncta in MB lobes. Images were first contrast enhanced using a brightness/contrast enhancement (saturated pixels set to 0.3% and normalized) followed by thresholding using the Bernsen method in the Auto Local Threshold function with a 25 – 50 pixel radius depending on image quality. Particles were considered puncta when they were 0.25 – 3.0 μm^2 in size and showed 0.25 - 1.0 circularity. To measure mean particle size in each sample, a polygon was drawn over the visible portion of each lobe in at least three sections for each lobe. From these subsamples we calculated a mean particle size for each lobe of each brain. Summary statistics can be found in Supplemental table S2B.

Behavioral assays

Y-maze: To measure changes in working memory, we employed a y-maze assay described by Lewis et al. (2017). We tracked the two-dimensional movement of individual *Drosophila* placed in small symmetrical Y-mazes using video recordings for ten 1-minute trials following two minutes of acclimation time in the maze. Observations took place between 08:45 and 11:00 and 14:00 to 16:00 when flies were most active. Male and female flies were run separately and the locations of genotypes in the 7 by 7 maze array were randomized for each set of trials. Assays were conducted in a dark room with each maze lit uniformly from below with a white LED array and capped with a clear Plexiglas coverslip. The overall movement of flies and visits to three unique arms consecutively were quantified using the Noldus Ethovision software. Spontaneous alternation behavior was measured by scoring three consecutive arm entries in a sliding window during for each of 10 trials. The alternation score was calculated as alternations divided by alternation attempts. Movement and alternation data were summed for each fly during each 1-minute trial and then averaged over ten trials for statistical analyses. Flies originating from three biological replicates were pooled for analysis (Supplementary table S3). The large samples sizes permitted the use of parametric tests, and we assessed differences in distance moved or alternation score across genotypes using ANOVA on a linear mixed-effects model (lmer function in R; Bates et al., 2015) that included replicate as a fixed effect. Flies that performed no alternations naturally did not have a percent alternation score and were removed from subsequent analysis. Males and females were analyzed separately. Flies were additionally assessed for the presence of bias for specific arms, calculated as a ratio of the mean number of entries into each arm over mean total entries and tested for significant variation from 0.333 using the Wilcoxon Signed Rank test. Interestingly, while females showed no arm biases, males overexpressing *TDP-43*^{WT} and OR-R controls showed a bias against arm B (*TDP-43*^{WT}, $\bar{x}$ = 0.307 ± 0.08, P < 0.0001; OR-R, $\bar{x}$ = 0.316 ± 0.13, P = 0.0038). *TDP-43*^{WT} also showed a bias for arm A ($\bar{x}$ = 0.352 ± 0.076, P = 0.0033), while OR-R controls showed a bias for arm C ($\bar{x}$ = 0.347 ± 0.113, P = 0.048). Although these analyses suggest that arm biases exist in males and

are not unique to TDP-43 overexpression, a single replicate was used to test whether Dlp over-expression could rescue alternation deficits seen in TDP-43 flies therefore hypothesis testing proceeded with non-parametric tests as described in *Statistical analyses*.

Sleep: Adult flies from the three age time points were monitored individually using Drosophila Activity Monitors (DAMs; Trikinetics, Waltham, MA; Chiu et al., 2010). Flies were placed in monitoring tubes with a small amount of food the day before they reached 2-3, 31-33, or 61-63 days old. Sleep and activity monitoring began at 12 AM following placement of flies in the sleep incubator, allowing flies at least six hours prior to the start of the experiment to acclimate to the tubes. Sleep and locomotor activity data were collected at 1-minute intervals for three days and analyzed using ShinyR-DAM (Cichewicz and Hirsh, 2018). In *Drosophila,* sleep is defined at 5 minutes of inactivity (Shaw et al., 2000) and here sleep data were processed using the ShinyR DAM program (Cichewicz and Hirsh 2018), which provided average sleep, sleep bout number and duration, and activity to sleep bout length ratio. Comparison of these variables by age and genotype were conducted separately for male and female flies. Data from two replicates were pooled.

Lifespan

Newly eclosed virgin males and females were separated and placed on fresh food, then transferred weekly into new food vials. The number of surviving flies was counted every other day for 100 days. Survival analysis and plots were generated using R packages *survival* (Therneau, 2021) and *survivminer* (Kassambara et al., 2021).

mRNA targets of TDP-43

RNA Immunoprecipitations: Equal numbers of male and female flies, aged 1-3 days, were pooled in Eppendorf tubes and flash frozen in liquid nitrogen. A minimum of 500 flies each expressing yellow fluorescent protein (YFP), *TDP-43*^{WT}-YFP, or *TDP-43*^{G298S}-YFP were

collected for three biological replicates. Frozen flies were then transferred to 50mL conical tubes and heads were separated from the bodies using four rounds of vortexing and flash freezing with liquid nitrogen. A sieve was used to filter out the bodies and isolated heads were collected into tubes containing lysis beads (Next Advance Green lysis beads). Heads were homogenized (Next Advance Bullet Blender) in 1mL fresh lysis buffer (DEPC water, 50 mM HEPES buffer pH 7.4, 0.5% Triton X-100, 150 mM NaCl, 30 mM EDTA), protease inhibitors (cOmplete™, Mini, EDTA-free Protease Inhibitor Cocktail, Millipore Sigma 11873580001), and RNAsin Plus 400 u/mL (Fischer Scientific PRN2615), centrifuged for 10 minutes at 10,000 rpm, and the lysate was collected. A portion of the lysate was saved for the protein input and RNA input samples. For protein input, the lysate was mixed with 2x Laemmli buffer, boiled at 95-100°C for 10 minutes, and stored at -20°C. For RNA input, TRIzol reagent (Thermofisher 15596026) was added to the lysate and the sample was stored at -80°C. High affinity GFP-Trap magnetic agarose beads (ChromoTek) were added to the remaining lysate and rotated end-over-end for 90 minutes at 4°C to allow for binding of YFP. The beads were separated from the lysate with a magnet and washed three times with fresh wash buffer (DEPC water, 50 mM HEPES buffer pH 7.4, 0.5% Triton X-100, 150 mM NaCl, 30 mM EDTA). The beads were resuspended in wash buffer and split into two tubes for the protein IP and RNA IP samples. For the protein IP sample, 2x Laemmli buffer was added to the beads, samples were boiled at 95-100°C for 10 minutes, and the beads were removed with a magnet. Western blots were performed to ensure that the immunoprecipitated complexes contained TDP-43 before processing the RNA IPs. For the RNA IP sample, TRIzol reagent was added to the beads, the solution was pipetted up and down for 60 seconds, and the beads were removed with a magnet.

RNA-Seq: RNA was quantified by nanodrop to bring it within range for ribogreen quantification. RNA was also checked using Agilent Tapestation High Sensitivitiy RNA screentape. 1 ng total RNA was used for SMART-Seq HT PLUS (Takara Bio USA, Inc. Cat # R400748) following manufacturer's protocol. Determination of cDNA quality and quantity was determined via Agilent

Tapestation High Sensitivity D5000 Screentape and Qubit dsDNA HS assay for input into library amplification. Libraries were quantified by Agilent Tapestation High Sensitivity D1000 Screentape and Kapa Library Quantification kit for Illumina platforms. Libraries were pooled equimolarly, pools were quantified by Agilent Tapestation High Sensitivity D1000 Screentape and Kapa Library Quantification kit and loaded on the NovaSeq 6000 S4 flowcell and sequenced to 101 x 11 x 11 x 101 cycles. Trimmed fastqs were aligned to the Dmel genome with STAR v2.6.1d (Dobin et al., 2013). Aligned reads were counted with featureCounts v1.6.3 (Liao et al., 2014) using the genome annotation. Files produced for individual samples were aggregated into a single .txt file using python. Differential expression was quantified using Deseq2 (Love et al., 2014). We included over-expression of cytoplasmic YFP in MBNs as a control for IPs, however the expression levels in the control condition were far greater than cytoplasmic TDP-43 YFP (data not shown), making it difficult to assess the role of cytoplasmic YFP alone. To ensure that candidate mRNA targets showing the greatest enrichment were indeed enriched in their association with TDP-43, we subtracted YFP control Log2FC values from the Log2FC values of targets recovered in each of our models. Indeed, in this YFP-subtracted analysis *futsch* was recovered as enriched with TDP-43 in both variants (Figure 6A, Figure 6-figure supplement 1A) and the majority of mRNAs that showed high enrichment in the original analysis were retained in the YFP-subtracted analyses (Figure 6A vs 6D, Supplemental figure S6A vs S6C).

Functional annotation: The Database for Annotation, Visualization, and Integrated Discovery (DAVID) was used to functionally annotated genes enriched with TDP-43 (Dennis et al., 2003; Sherman et al., 2022). To assess genes over-represented in our disease model data sets, we used lists of genes significantly enriched with each of our TDP-43 models against a background of all genes identified from models and controls.

RNA Extraction for Validation: RNA input and RNA IP samples, stored in TRIzol reagent (Thermofisher 15596026) at -80°C, were allowed to thaw completely on ice and chloroform was

added to each sample. Samples were shaken briefly to mix, left to incubate for 3 minutes at room temperature, and then centrifuged at 12,000 rpm for 15 minutes at 4°C to allow for separation of the aqueous and organic phases. The RNA-containing aqueous phase was collected and molecular grade isopropyl alcohol was added to each sample. Samples were incubated for 10 minutes at room temperature for RNA precipitation and then centrifuged at 12,000 rpm for 10 minutes. The pelleted RNA was washed with 75% ethanol (200 proof ethanol & HyPure water) and left to dry in a fume hood. RNA was resuspended in HyPure water and the concentration and 260/280 absorbance ratio were measured using Nanodrop.

RT-qPCR: RNA extracted from input and IP samples was used as template RNA for cDNA synthesis by reverse transcription. Total RNA used in the cDNA synthesis reactions was normalized across samples. cDNA was synthesized using the Fisher First Strand cDNA synthesis kit (Thermofisher Scientific K1641). qPCR reactions were prepared in a 96-well qPCR plate, in triplicates, using Taqman Fast Advanced Master Mix (Thermofisher Scientific 4444556) and Taqman probes for Dally-like protein (dlp) (Thermofisher Scientific Dm01798597_m1) and Gpdh1 (Thermofisher Scientific Dm01841185_m1). qPCR was conducted on the qTOWER (Analytik Jena 844-00504-4) qPCR machine. Delta Ct was calculated as the difference in Ct values (dlp - gpdh1). To determine enrichment of dlp mRNA in the IPs, ΔΔCt was calculated as the difference in Delta Ct values (IP - Input). Fold change was calculated as 2^(-ΔΔCt).

Dally-like protein target validation: Brains from flies 1-3 days or 50-55 days were dissected out and the tissue fixed, permeabilized and blocked as described above. Brains were then incubated overnight at 4°C in an anti-Dally-like protein antibody at 1:5 in block (13G8 developed by Phil Beachy, obtained from the Developmental Studies Hybridoma Bank, created by the NICHD of the NIH and maintained at The University of Iowa, Department of Biology, Iowa City, IA 52242, targets amino acids V523 to Q702), rinsed 3X in 0.1% PBST and incubated in goat anti-mouse Alexa Flour 647 antibody overnight at 4°C (1:300, ThermoFisher A32728). Images were acquired using a Zeiss 880 Laser Scanning Confocal inverted microscope with a Plan-

Apochromat 63x/1.4 oil DIC M27 lens. Signal intensity was traced from maximum intensity projections of the MBLs and normalized to background intensity. Dlp signal intensity declined with age in TDP-43 flies, so the mCD8-RFP channel was used to trace the lobes in aged brains, ensuring the correct lobe area was used for signal intensity measurements.

ACKNOWLEDGEMENTS

We would like to thank Patty Jansma at the University of Arizona Imaging Cores - Optical Facility for her consultation on sample preparation and image acquisition and Dr. Shaun Davis in the Schlenke lab for generating TDP-43 transgenic lines in a OR-R background. We also acknowledge Dr. Robert Kraft for generating UAS TDP-43; UAS RFP stocks. We thank Dr. Yoshi Aso for sharing the SS01276 GAL4 line and Dr. Fabian Fernandez for Y maze training. Support for Hillary Cowell was provided in part by The University of Arizona's Undergraduate Research Opportunities Consortium Prep (UROC-Prep) Program. The University of Arizona Maximizing Access to Research Careers (MARC Training Grant NIGMS T34 GM008718) program provided support for Grace Hala'ufia. We would like to acknowledge Suvitha Loganathan, Samantha Macklin-Isquierdo in the Zarnescu lab for their advice on experimental design and data analysis, and feedback on the manuscript.

Figure

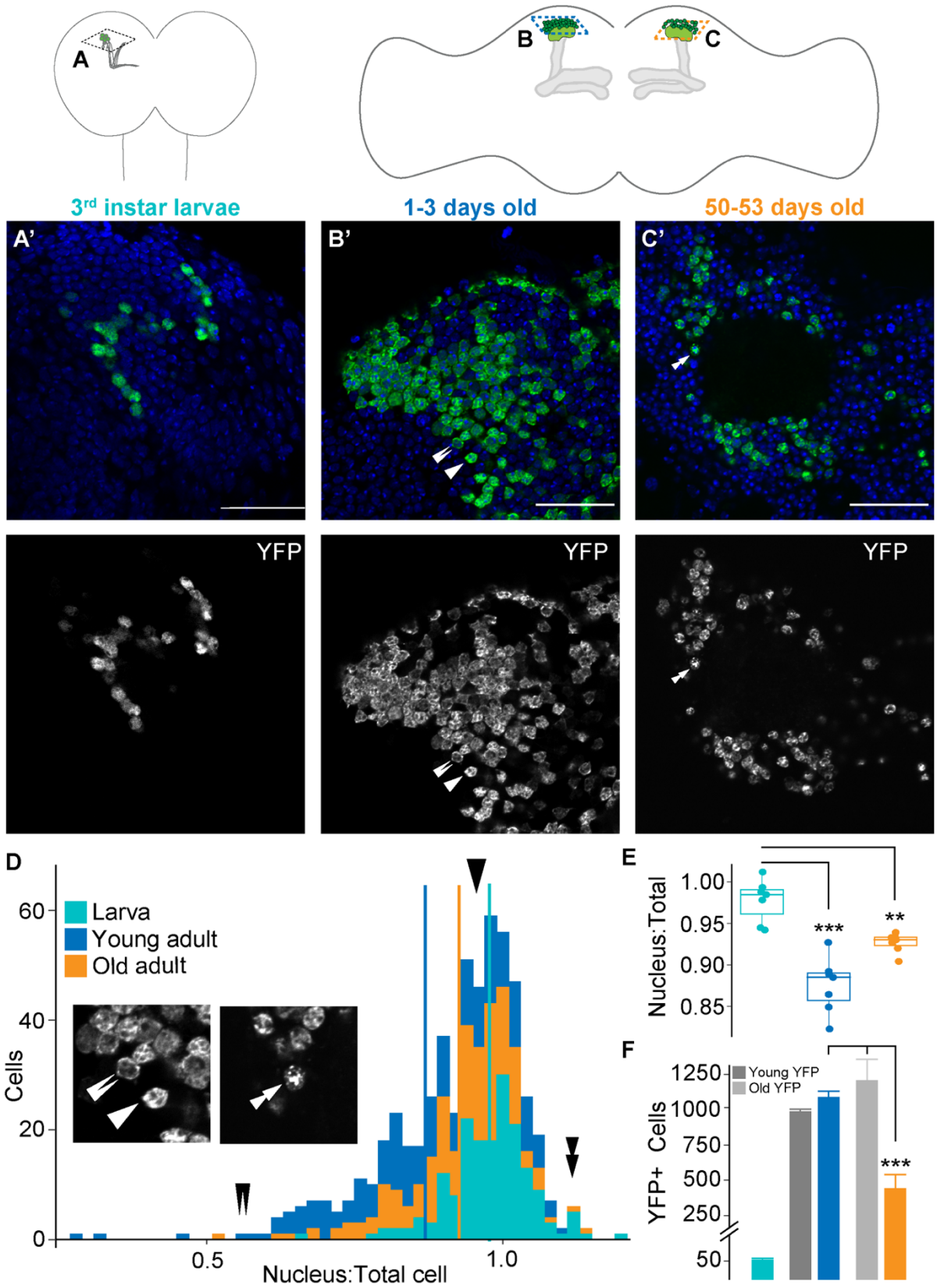
A
B
C
3rd instar larvae
1-3 days old
50-53 days old
A'
B'
C'
YFP
YFP
YFP
D
Larva
Young adult
Old adult
Cells
Nucleus:Total cell
0
20
40
60
0.5
1.0
E
Nucleus:Total
1.00
0.95
0.90
0.85
***
**
F
Young YFP
Old YFP
YFP+ Cells
1250
1000
750
500
250
50
***

Figure 1. *TDP-43*^{WT} overexpression in Kenyon Cells results in cytoplasmic mis-localization and age-dependent cell loss. Illustrations in (A), (B), and (C) correspond to approximate plane of imaging for Kenyon cells in (A') larval brain, (B') young adult brain, and (C') old adult brain. (A') Nuclear localization of human wild-type *TDP-43*^{WT} in the larval MBNs. (B') Young adult flies (1 – 3 days) contain cells with *TDP-43*^{WT} in the cell body and cells showing nuclear loss of TDP-43 (adjacent, double arrows as compared with single arrow). (C') Old adults (50 – 55 days) have fewer cells with nuclear depletion but concurrent loss in total number of *TDP-43*^{WT} positive neurons (quantified in E and F). Stacked, double arrows indicate a cell that has a signal intensity ratio > 1 due to punctate TDP-43 signal in the nucleus. (D) Histograms showing distribution of *TDP-43*^{WT} signal intensity ratios (cell nuclei to total cell) shift with age. Arrows correspond to measurements taken from cells shown in figure inset taken from (B'), (C'). (E) Age-specific *TDP-43*^{WT} signal intensity ratios. (F) Decrease in *TDP-43*^{WT} positive cells from young to old adults. Larval cell numbers provided for reference, but not used in statistical comparisons. Data for *TDP-43*^{G298S} presented in Figure1-supplement 1. Scale bar = 50 μm. ** = $P < 0.01$; *** = $P < 0.001$.

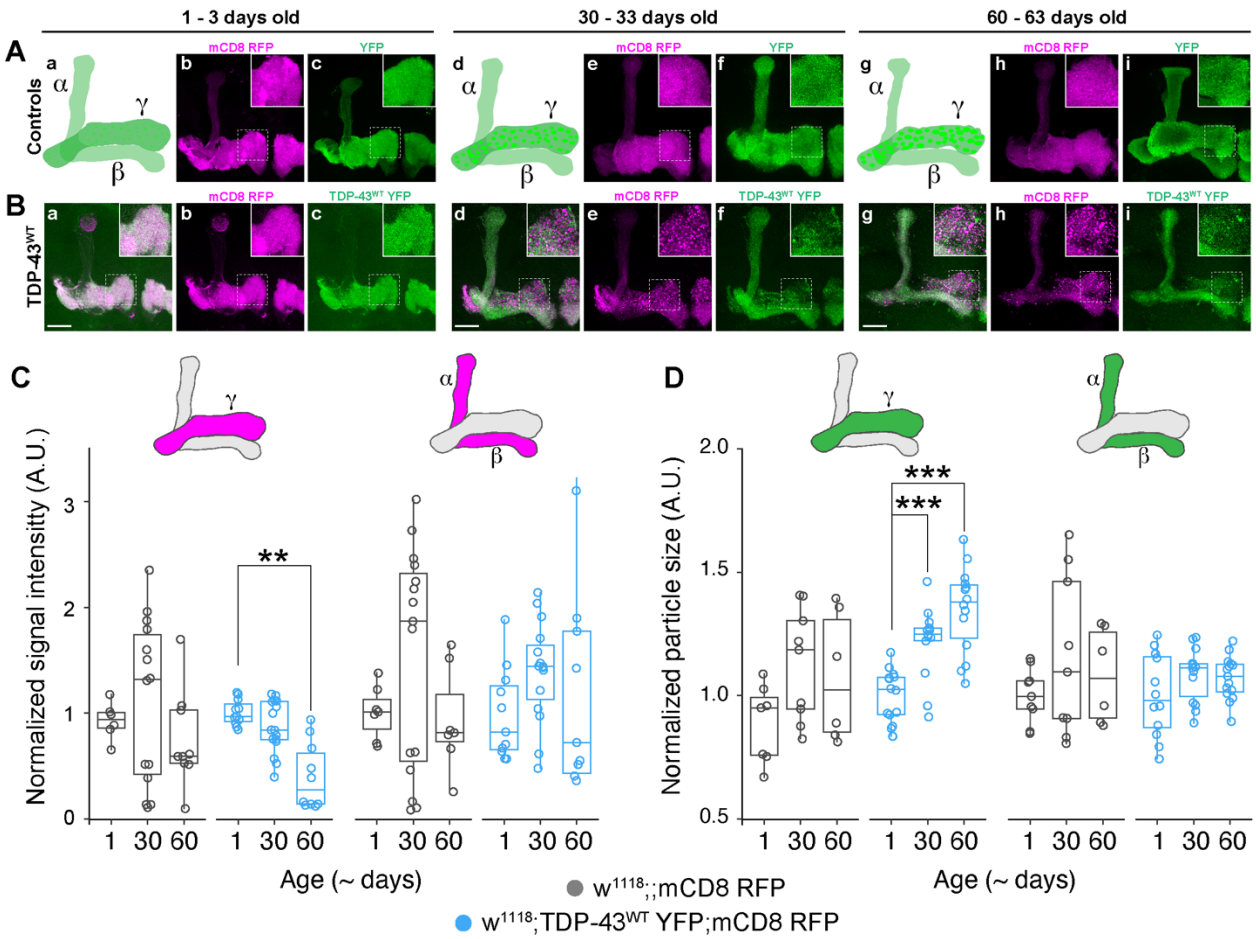

Figure 2. Mushroom body lobes (MBLs) show age-related, region-specific *TDP-43^{WT}* accumulation and axonal fragmentation. (A) Illustrations of changes in MBLs targeted by *TDP-43^{WT}* OE over time (a, d, g) alongside morphology of young (b, c,) middle-aged (e, f) and old (h, i) control flies expressing membrane-bound RFP or cytoplasmic YFP. (B) Over expression of *TDP-43^{WT}* in MBNs results in axonal localization of TDP-43 in young adult flies (c) and dystrophic neurites in middle-aged (e) and old (h) flies. (D) Signal intensity of RFP with age in γ and α/β lobes. (E) Changes in YFP particle size with age in γ and α/β lobes. Data for *TDP-43^{G298S}* presented in Figure 2-supplement 1. Scale bar = 25 μm * = P <0.05; ** = P < 0.01; *** = P < 0.001.

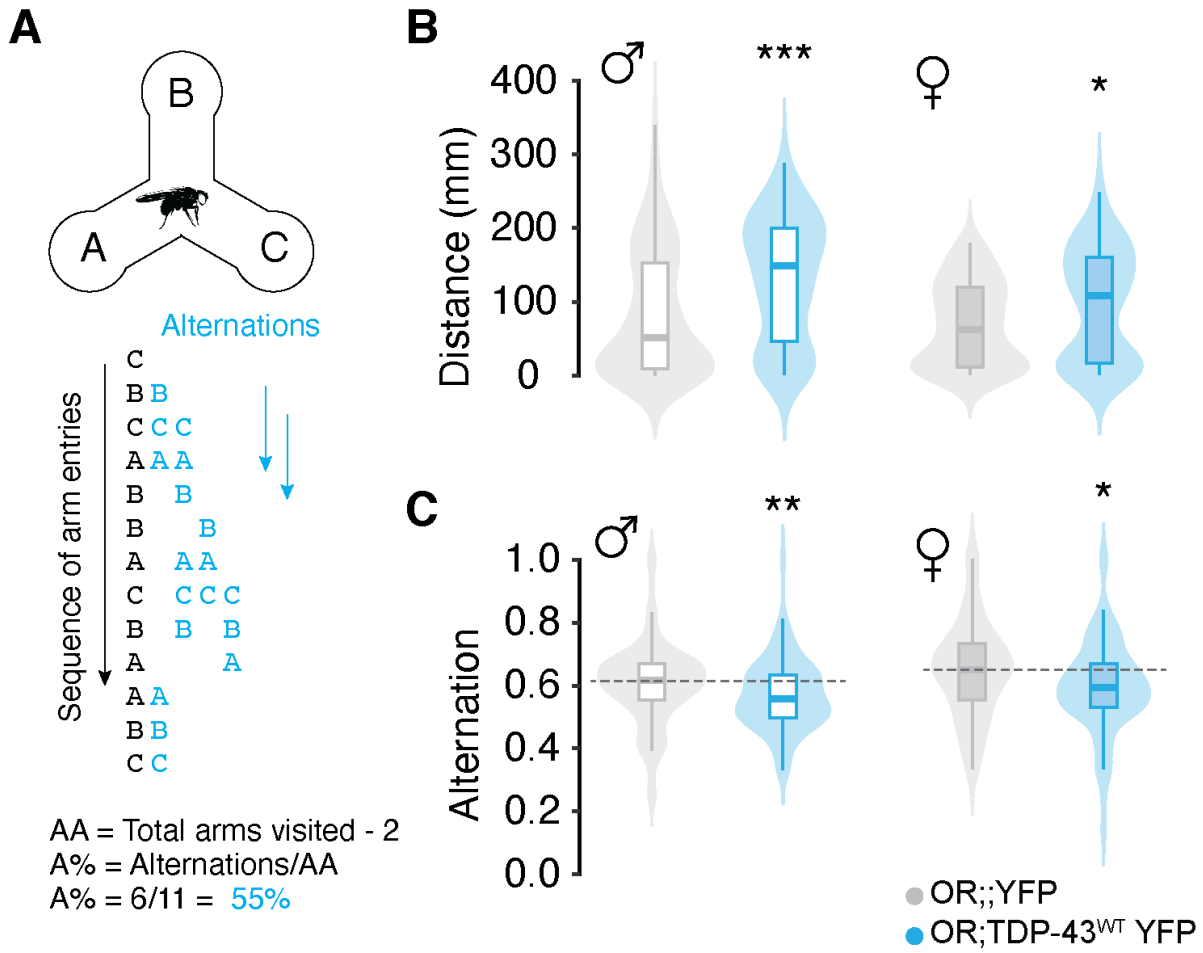

Figure 3. Overexpression of TDP-43 in mushroom body MBNs results in spatial working memory deficits. (A) Schematic of the spatial working memory assay showing the sequence of decisions made by a fly (black text) and those coded as alternations (blue text). Percent alternation calculated as alternations divided by alternation attempts (AA). (B) Young (1-3 days old) flies with *TDP-43*^{WT} OE show significant increases in movement. (C) Despite moving more, these flies show reduced alternation percent when compared with controls. Grey dotted line = control group median. AA = alternation attempts. A% = alternation percent. * = P <0.05; ** = P < 0.01; *** = P < 0.001.

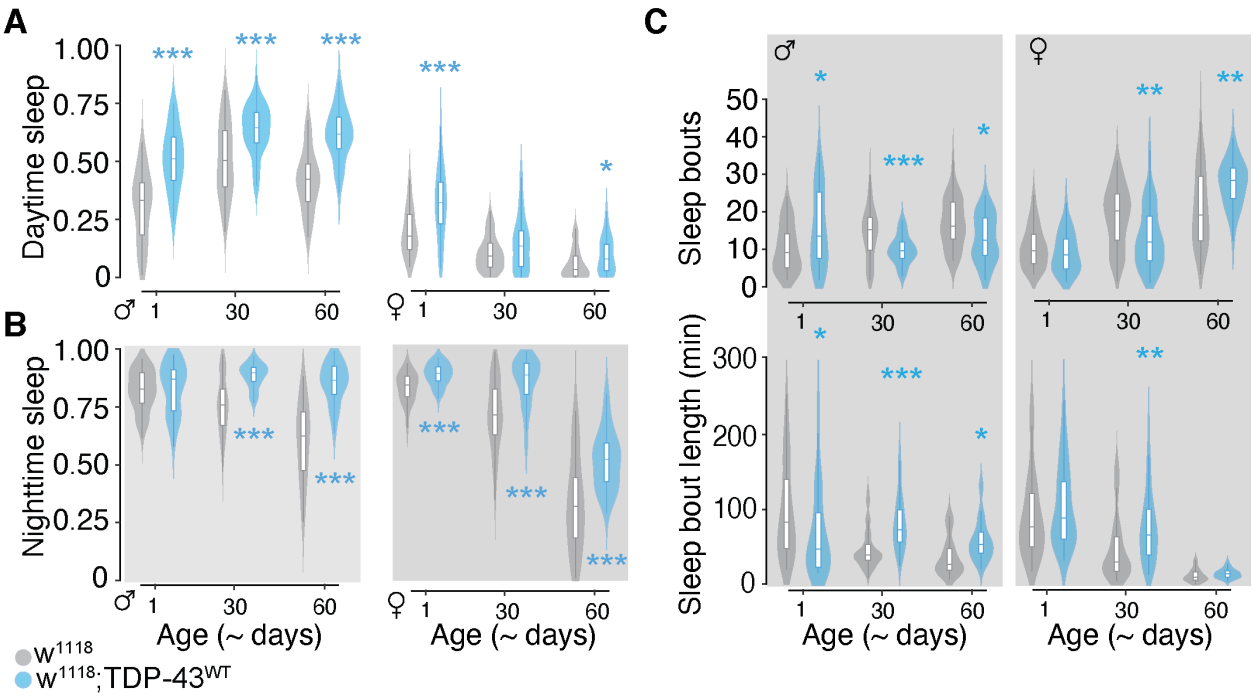

Figure 4. *TDP-43^{WT}* overexpression in mushroom body MBNs reduces arousal, increasing day and night sleep. (A) Proportion of time flies spent sleeping during the day and (B) at night. (C) Sleep fragmentation assessed by number of sleep bouts (top panel) and mean bout length (bottom panel) during the night. Male data on the left and female data on the right in each panel. Data for *TDP-43^{G298S}* presented in Figure 4-supplement 1. * = P <0.05; ** = P < 0.01; *** = P < 0.001.

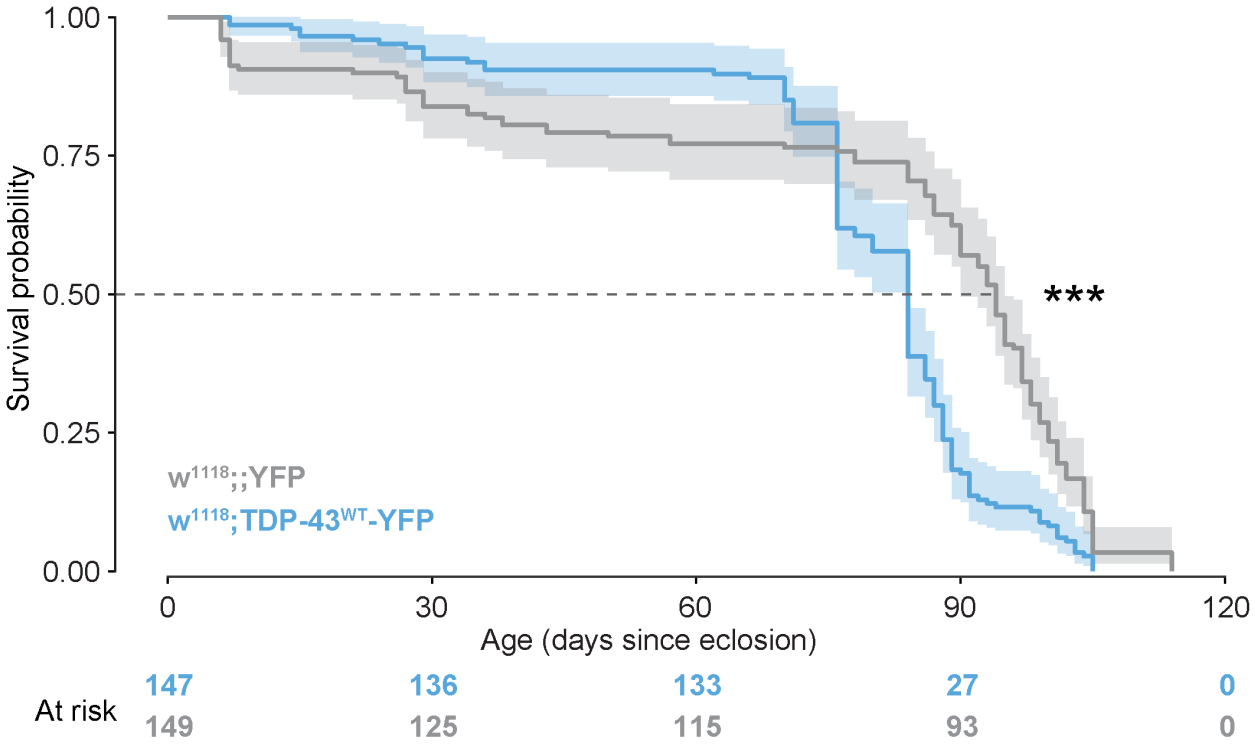

Figure 5. TDP-43 overexpression in MBs is sufficient to reduce lifespan. Data from male and female flies pooled for analysis. Number of flies N=149 for YFP controls and 147 for TDP-43^{WT} – YFP expressing flies), Data for *TDP-43*^{G298S} presented in Figure 5-supplement 1. *** P < 0.001.

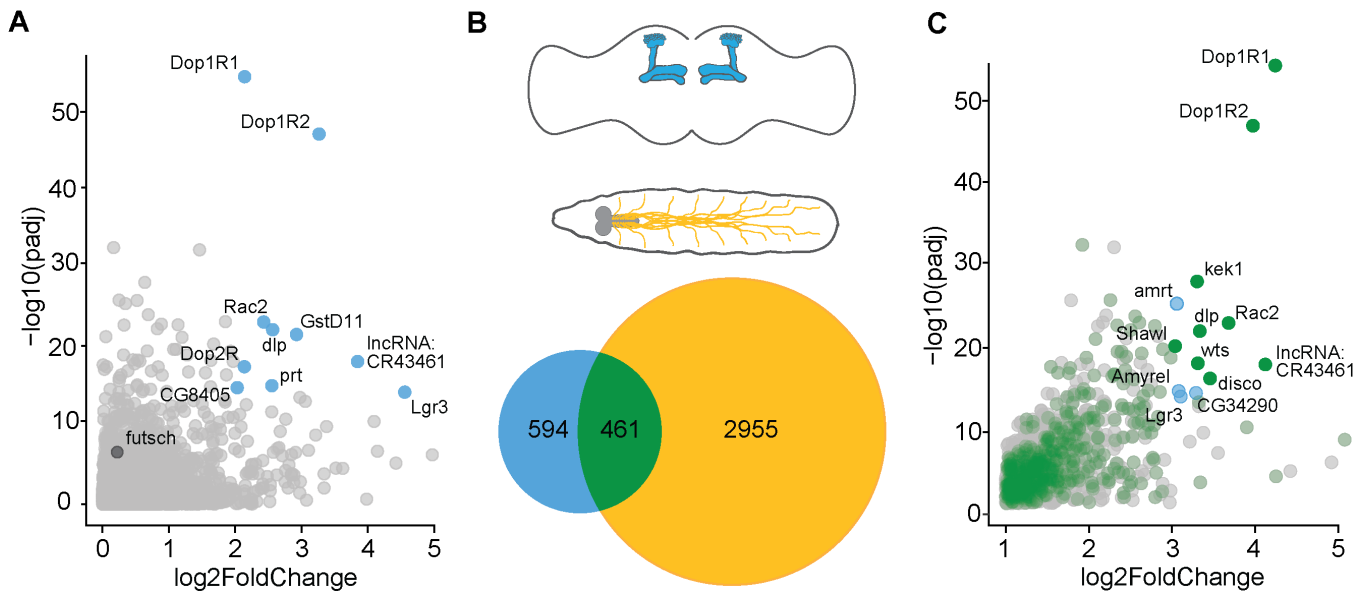

Figure 6. mRNAs enriched with TDP-43 *Drosophila* models of FTD and ALS. (A) Volcano plot displaying mRNAs enriched with TDP-43. Y-axis depicts Log2 fold change after subtraction of YFP control values; Blue circles indicate log2 fold change > 2 and $P < 1 \times 10^{-14}$. (B) Schematic showing subsets of neurons in fly model of FTD (MBs, above) and ALS (below), and Venn diagram depicting enriched mRNAs unique to and overlapping between models. (C) Volcano plot displaying mRNAs enriched in TDP-43 complexes that are shared between MB and MN models (green); saturated green circles indicate shared targets that show log2 fold change > 3 and $P < 1 \times 10^{-14}$; blue circles indicate MB targets with log2 fold change > 2 and $P < 1 \times 10^{-14}$. Data for *TDP-43*^{G298S} presented in Figure 6-supplement 1.

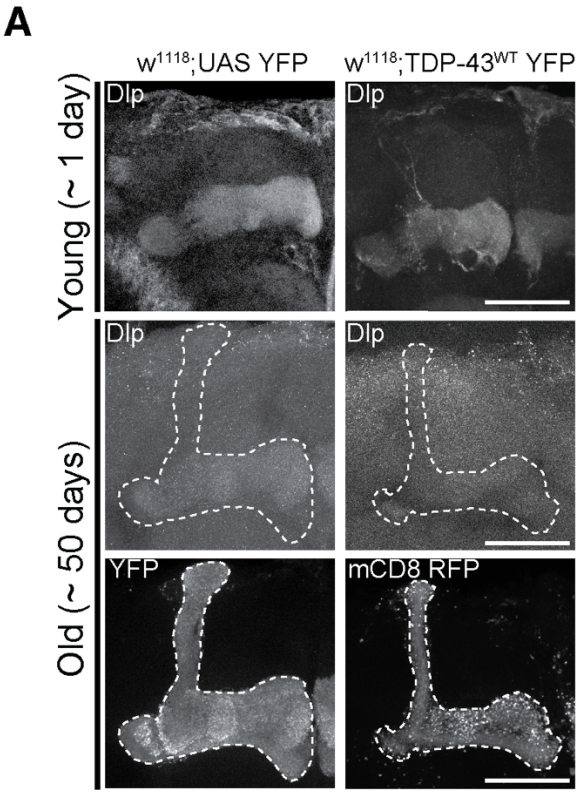
A
w1118;UAS YFP
w1118;TDP-43WT YFP
Young (~ 1 day)
Old (~ 50 days)
Dlp
YFP
mCD8 RFP

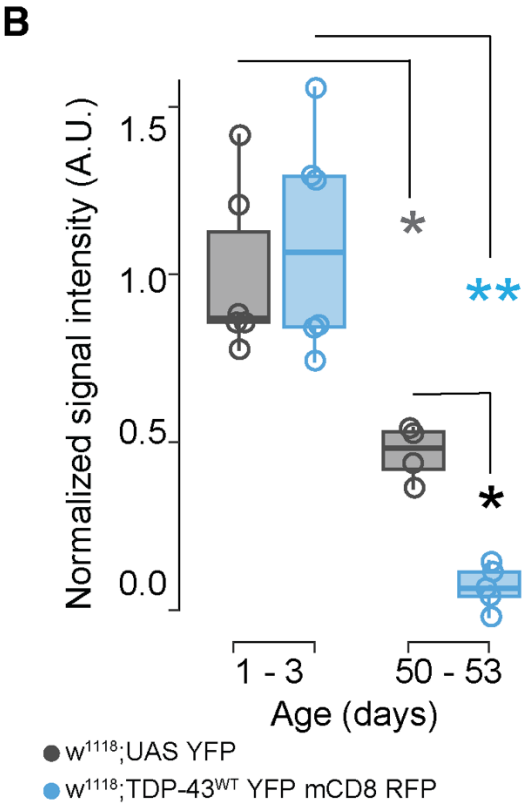
B
Normalized signal intensity (A.U.)
1.5
1.0
0.5
0.0
*
**
*
1 - 3
50 - 53
Age (days)
w1118;UAS YFP
w1118;TDP-43WT YFP mCD8 RFP

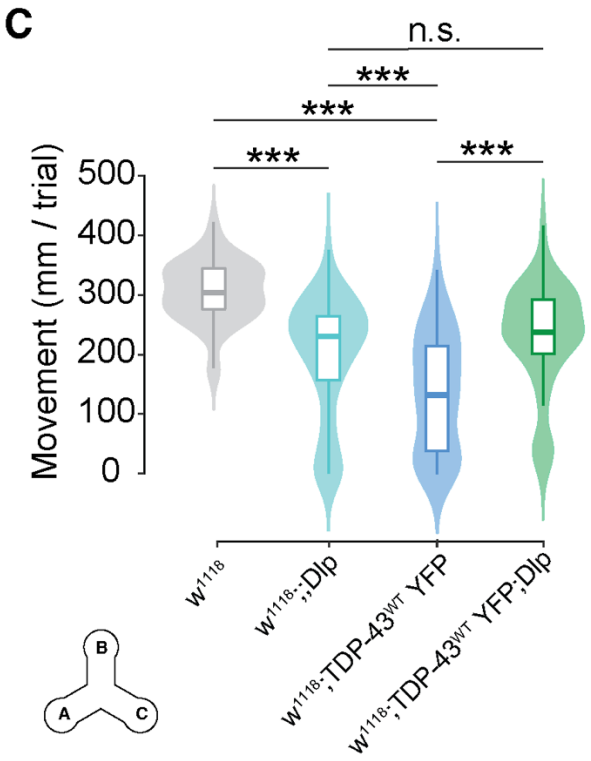
C
Movement (mm / trial)
500
400
300
200
100
0
n.s.
***
***
***
***
w1118
w1118;;Dlp
w1118;TDP-43WT YFP
w1118;TDP-43WT YFP;Dlp
A
B
C

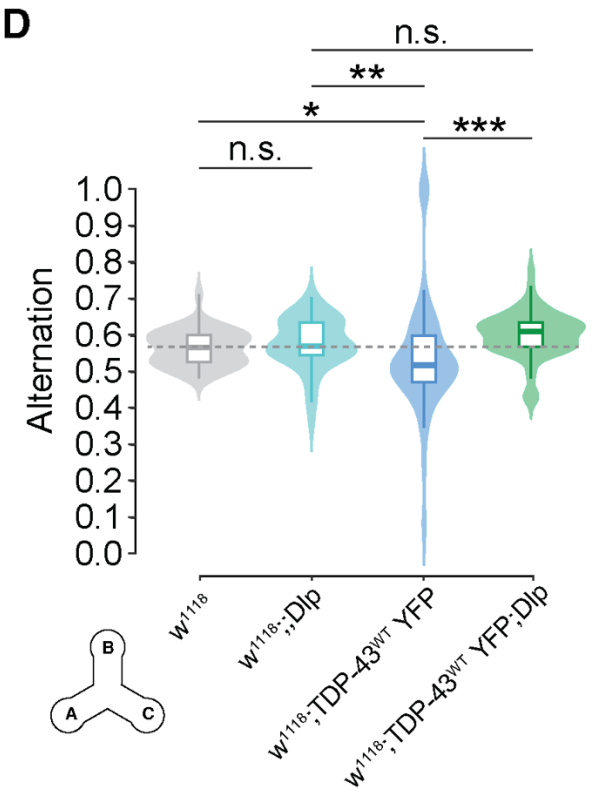
D
Alternation
1.0
0.9
0.8
0.7
0.6
0.5
0.4
0.3
0.2
0.1
0.0
n.s.
**
*
n.s.
***
w1118
w1118;;Dlp
w1118;TDP-43WT YFP
w1118;TDP-43WT YFP;Dlp
A
B
C

Figure 7. Dally-like protein is a target of TDP-43^{WT} in MBNs where it mediates TDP-43 dependent working memory deficits. (A) Age-dependent loss of Dlp antibody labelling in mushroom bodies. Cytoplasmic YFP (Control) or mCD8 RFP (TDP OE genotypes) in aged flies indicating intact MBLs show decreased Dlp signal at ~ 50 days. (B) Change in Dlp signal intensity in MBLs with age. Scale bar = 50 μm. (C) Mean distance moved and (D) alternation per trail in males. Grey dotted line represents control group median. Data for *TDP-43*^{G298S} presented in Figure 7-supplement 1. * = P < 0.05, ** = P < 0 .01.

REFERENCES

Al-Chalabi, A., Jones, A., Troakes, C., King, A., Al-Sarraj, S., and van den Berg, L.H. (2012). The genetics and neuropathology of amyotrophic lateral sclerosis. Acta Neuropathol *124*, 339-352. 10.1007/s00401-012-1022-4.

Alami, N.H., Smith, R.B., Carrasco, M.A., Williams, L.A., Winborn, C.S., Han, S.S., Kiskinis, E., Winborn, B., Freibaum, B.D., Kanagaraj, A., et al. (2014). Axonal transport of TDP-43 mRNA granules is impaired by ALS-causing mutations. Neuron *81*, 536-543. 10.1016/j.neuron.2013.12.018.

Altman, T., Ionescu, A., Ibraheem, A., Priesmann, D., Gradus-Pery, T., Farberov, L., Alexandra, G., Shelestovich, N., Dafinca, R., Shomron, N., et al. (2021). Axonal TDP-43 condensates drive neuromuscular junction disruption through inhibition of local synthesis of nuclear encoded mitochondrial proteins. Nat Commun *12*, 6914. 10.1038/s41467-021-27221-8.

Amador-Ortiz, C., Lin, W.L., Ahmed, Z., Personett, D., Davies, P., Duara, R., Graff-Radford, N.R., Hutton, M.L., and Dickson, D.W. (2007). TDP-43 immunoreactivity in hippocampal sclerosis and Alzheimer's disease. Ann Neurol *61*, 435-445. 10.1002/ana.21154.

Arai, T., Hasegawa, M., Akiyama, H., Ikeda, K., Nonaka, T., Mori, H., Mann, D., Tsuchiya, K., Yoshida, M., Hashizume, Y., and Oda, T. (2006). TDP-43 is a component of ubiquitin-positive tau-negative inclusions in frontotemporal lobar degeneration and amyotrophic lateral sclerosis. Biochem Biophys Res Commun *351*, 602-611. 10.1016/j.bbrc.2006.10.093.

Ash, P.E., Zhang, Y.J., Roberts, C.M., Saldi, T., Hutter, H., Buratti, E., Petrucelli, L., and Link, C.D. (2010). Neurotoxic effects of TDP-43 overexpression in C. elegans. Hum Mol Genet *19*, 3206-3218. 10.1093/hmg/ddq230.

Aso, Y. (2021). Split-GAL4 Mushroom Body Driver Line

Aso, Y., Grubel, K., Busch, S., Friedrich, A.B., Siwanowicz, I., and Tanimoto, H. (2009). The mushroom body of adult Drosophila characterized by GAL4 drivers. J Neurogenet *23*, 156-172. 10.1080/01677060802471718.

Aso, Y., Hattori, D., Yu, Y., Johnston, R.M., Iyer, N.A., Ngo, T.T., Dionne, H., Abbott, L.F., Axel, R., Tanimoto, H., and Rubin, G.M. (2014). The neuronal architecture of the mushroom body provides a logic for associative learning. Elife *3*, e04577. 10.7554/eLife.04577.

Ayala, Y.M., Pantano, S., D'Ambrogio, A., Buratti, E., Brindisi, A., Marchetti, C., Romano, M., and Baralle, F.E. (2005). Human, Drosophila, and C.elegans TDP43: nucleic acid binding properties and splicing regulatory function. J Mol Biol *348*, 575-588. 10.1016/j.jmb.2005.02.038.

Azpurua, J., El-Karim, E.G., Tranquille, M., and Dubnau, J. (2021). A behavioral screen for mediators of age-dependent TDP-43 neurodegeneration identifies SF2/SRSF1 among a group

of potent suppressors in both neurons and glia. PLoS Genet *17*, e1009882. 10.1371/journal.pgen.1009882.

Baier, A., Wittek, B., and Brembs, B. (2002). Drosophila as a new model organism for the neurobiology of aggression? J Exp Biol *205*, 1233-1240. 10.1242/jeb.205.9.1233.

Bates, D., Mächler, M., Bolker, B., and Walker, S. (2015). Fitting Linear Mixed-Effects Models Usinglme4. Journal of Statistical Software *67*. 10.18637/jss.v067.i01.

Bellen, H.J. (1998). The fruit fly: a model organism to study the genetics of alcohol abuse and addiction? Cell *93*, 909-912. 10.1016/s0092-8674(00)81195-2.

Benjamini, Y., and Hochberg, Y. (1995). Controlling the False Discovery Rate A Practical and Powerful Approach to Multiple Testing. Journal of the Royal Statistical Society. Series B (Methodological) *57*, 289-300.

Bier, E. (2005). Drosophila, the golden bug, emerges as a tool for human genetics. Nat Rev Genet *6*, 9-23. 10.1038/nrg1503.

Bjork, R.T., Mortimore, N.P., Loganathan, S., and Zarnescu, D.C. (2022). Dysregulation of Translation in TDP-43 Proteinopathies: Deficits in the RNA Supply Chain and Local Protein Production. Front Neurosci *16*, 840357. 10.3389/fnins.2022.840357.

Bonakis, A., Economou, N.T., Paparrigopoulos, T., Bonanni, E., Maestri, M., Carnicelli, L., Di Coscio, E., Ktonas, P., Vagiakis, E., Theodoropoulos, P., and Papageorgiou, S.G. (2014). Sleep in frontotemporal dementia is equally or possibly more disrupted, and at an earlier stage, when compared to sleep in Alzheimer's disease. J Alzheimers Dis *38*, 85-91. 10.3233/JAD-122014.

Borroni, B., Bonvicini, C., Alberici, A., Buratti, E., Agosti, C., Archetti, S., Papetti, A., Stuani, C., Di Luca, M., Gennarelli, M., and Padovani, A. (2009). Mutation within TARDBP leads to Frontotemporal Dementia without motor neuron disease. Human Mutation *30*, E974-E983. 10.1002/humu.21100.

Bridi, J.C., Ludlow, Z.N., Kottler, B., Hartmann, B., Vanden Broeck, L., Dearlove, J., Goker, M., Strausfeld, N.J., Callaerts, P., and Hirth, F. (2020). Ancestral regulatory mechanisms specify conserved midbrain circuitry in arthropods and vertebrates. Proc Natl Acad Sci U S A *117*, 19544-19555. 10.1073/pnas.1918797117.

Cairns, N.J., Neumann, M., Bigio, E.H., Holm, I.E., Troost, D., Hatanpaa, K.J., Foong, C., White, C.L., 3rd, Schneider, J.A., Kretzschmar, H.A., et al. (2007). TDP-43 in familial and sporadic frontotemporal lobar degeneration with ubiquitin inclusions. Am J Pathol *171*, 227-240. 10.2353/ajpath.2007.070182.

Chakraborty, R., Vepuri, V., Mhatre, S.D., Paddock, B.E., Miller, S., Michelson, S.J., Delvadia, R., Desai, A., Vinokur, M., Melicharek, D.J., et al. (2011). Characterization of a Drosophila

Alzheimer's disease model: pharmacological rescue of cognitive defects. PLoS One *6*, e20799. 10.1371/journal.pone.0020799.

Chang, X.-L., Tan, M.-S., Tan, L., and Yu, J.-T. (2015). The Role of TDP-43 in Alzheimer's Disease. Molecular Neurobiology *53*, 3349-3359. 10.1007/s12035-015-9264-5.

Chen, H.J., Topp, S.D., Hui, H.S., Zacco, E., Katarya, M., McLoughlin, C., King, A., Smith, B.N., Troakes, C., Pastore, A., and Shaw, C.E. (2019). RRM adjacent TARDBP mutations disrupt RNA binding and enhance TDP-43 proteinopathy. Brain *142*, 3753-3770. 10.1093/brain/awz313.

Chen, Y., Guan, Y., Zhang, Z., Liu, H., Wang, S., Yu, L., Wu, X., and Wang, X. (2013). Wnt signaling pathway is involved in the pathogenesis of amyotrophic lateral sclerosis in adult transgenic mice. Neurological Research *34*, 390-399. 10.1179/1743132812y.0000000027.

Chiu, J.C., Low, K.H., Pike, D.H., Yildirim, E., and Edery, I. (2010). Assaying locomotor activity to study circadian rhythms and sleep parameters in Drosophila. J Vis Exp. 10.3791/2157.

Chou, C.-C., Zhang, Y., Umoh, M.E., Vaughan, S.W., Lorenzini, I., Liu, F., Sayegh, M., Donlin-Asp, P.G., Chen, Y.H., Duong, D.M., et al. (2018). TDP-43 pathology disrupts nuclear pore complexes and nucleocytoplasmic transport in ALS/FTD. Nature Neuroscience *21*, 228-239. 10.1038/s41593-017-0047-3.

Cichewicz, K., and Hirsh, J. (2018). ShinyR-DAM: a program analyzing Drosophila activity, sleep and circadian rhythms. Commun Biol *1*, 25. 10.1038/s42003-018-0031-9.

Colombrita, C., Zennaro, E., Fallini, C., Weber, M., Sommacal, A., Buratti, E., Silani, V., and Ratti, A. (2009). TDP-43 is recruited to stress granules in conditions of oxidative insult. J Neurochem *111*, 1051-1061. 10.1111/j.1471-4159.2009.06383.x.

Coyne, A.N., Lorenzini, I., Chou, C.C., Torvund, M., Rogers, R.S., Starr, A., Zaepfel, B.L., Levy, J., Johannesmeyer, J., Schwartz, J.C., et al. (2017). Post-transcriptional Inhibition of Hsc70-4/HSPA8 Expression Leads to Synaptic Vesicle Cycling Defects in Multiple Models of ALS. Cell Rep *21*, 110-125. 10.1016/j.celrep.2017.09.028.

Coyne, A.N., Siddegowda, B.B., Estes, P.S., Johannesmeyer, J., Kovalik, T., Daniel, S.G., Pearson, A., Bowser, R., and Zarnescu, D.C. (2014). Futsch/MAP1B mRNA is a translational target of TDP-43 and is neuroprotective in a Drosophila model of amyotrophic lateral sclerosis. J Neurosci *34*, 15962-15974. 10.1523/JNEUROSCI.2526-14.2014.

Coyne, A.N., Yamada, S.B., Siddegowda, B.B., Estes, P.S., Zaepfel, B.L., Johannesmeyer, J.S., Lockwood, D.B., Pham, L.T., Hart, M.P., Cassel, J.A., et al. (2015). Fragile X protein mitigates TDP-43 toxicity by remodeling RNA granules and restoring translation. Hum Mol Genet *24*, 6886-6898. 10.1093/hmg/ddv389.

Crittenden (1998). Tripartite Mushroom Body Architecture Revealed by Antigenic Markers.

de Belle, J.S., and Heisenberg, M. (1994). Associative odor learning in Drosophila abolished by chemical ablation of mushroom bodies. Science *263*, 692-695. 10.1126/science.8303280.

Dennis, G., Jr., Sherman, B.T., Hosack, D.A., Yang, J., Gao, W., Lane, H.C., and Lempicki, R.A. (2003). DAVID: Database for Annotation, Visualization, and Integrated Discovery. Genome Biol *4*, P3.

Dobin, A., Davis, C.A., Schlesinger, F., Drenkow, J., Zaleski, C., Jha, S., Batut, P., Chaisson, M., and Gingeras, T.R. (2013). STAR: ultrafast universal RNA-seq aligner. Bioinformatics *29*, 15-21. 10.1093/bioinformatics/bts635.

Driscoll, M., Buchert, S.N., Coleman, V., McLaughlin, M., Nguyen, A., and Sitaraman, D. (2021). Compartment specific regulation of sleep by mushroom body requires GABA and dopaminergic signaling. Sci Rep *11*, 20067. 10.1038/s41598-021-99531-2.

Elden, A.C., Kim, H.J., Hart, M.P., Chen-Plotkin, A.S., Johnson, B.S., Fang, X., Armakola, M., Geser, F., Greene, R., Lu, M.M., et al. (2010). Ataxin-2 intermediate-length polyglutamine expansions are associated with increased risk for ALS. Nature *466*, 1069-1075. 10.1038/nature09320.

Enell, L.E., Kapan, N., Soderberg, J.A., Kahsai, L., and Nassel, D.R. (2010). Insulin signaling, lifespan and stress resistance are modulated by metabotropic GABA receptors on insulin producing cells in the brain of Drosophila. PLoS One *5*, e15780. 10.1371/journal.pone.0015780.

Erwin, D.H. (2015). Early metazoan life: divergence, environment and ecology. Philos Trans R Soc Lond B Biol Sci *370*. 10.1098/rstb.2015.0036.

Estes, P.S., Boehringer, A., Zwick, R., Tang, J.E., Grigsby, B., and Zarnescu, D.C. (2011). Wild-type and A315T mutant TDP-43 exert differential neurotoxicity in a Drosophila model of ALS. Hum Mol Genet *20*, 2308-2321. 10.1093/hmg/ddr124.

Estes, P.S., Daniel, S.G., McCallum, A.P., Boehringer, A.V., Sukhina, A.S., Zwick, R.A., and Zarnescu, D.C. (2013). Motor neurons and glia exhibit specific individualized responses to TDP-43 expression in a Drosophila model of amyotrophic lateral sclerosis. Dis Model Mech *6*, 721-733. 10.1242/dmm.010710.

Fallini, C., Bassell, G.J., and Rossoll, W. (2012). The ALS disease protein TDP-43 is actively transported in motor neuron axons and regulates axon outgrowth. Hum Mol Genet *21*, 3703-3718. 10.1093/hmg/dds205.

Feiguin, F., Godena, V.K., Romano, G., D'Ambrogio, A., Klima, R., and Baralle, F.E. (2009). Depletion of TDP-43 affects Drosophila motoneurons terminal synapsis and locomotive behavior. FEBS Lett *583*, 1586-1592. 10.1016/j.febslet.2009.04.019.

Ferrari, R., Kapogiannis, D., Huey, E.D., and Momeni, P. (2011). FTD and ALS: a tale of two diseases. Curr Alzheimer Res *8*, 273-294. 10.2174/156720511795563700.

Fiesel, F.C., Weber, S.S., Supper, J., Zell, A., and Kahle, P.J. (2012). TDP-43 regulates global translational yield by splicing of exon junction complex component SKAR. Nucleic Acids Res *40*, 2668-2682. 10.1093/nar/gkr1082.

Freibaum, B.D., Chitta, R.K., High, A.A., and Taylor, J.P. (2010). Global analysis of TDP-43 interacting proteins reveals strong association with RNA splicing and translation machinery. J Proteome Res *9*, 1104-1120. 10.1021/pr901076y.

Gao, J., Wang, L., Huntley, M.L., Perry, G., and Wang, X. (2018). Pathomechanisms of TDP-43 in neurodegeneration. J Neurochem. 10.1111/jnc.14327.

Gonzalez-Fernandez, C., Gonzalez, P., Andres-Benito, P., Ferrer, I., and Rodriguez, F.J. (2019). Wnt Signaling Alterations in the Human Spinal Cord of Amyotrophic Lateral Sclerosis Cases: Spotlight on Fz2 and Wnt5a. Mol Neurobiol *56*, 6777-6791. 10.1007/s12035-019-1547-9.

Graham, A., Davies, R., Xuereb, J., Halliday, G., Kril, J., Creasey, H., Graham, K., and Hodges, J. (2005). Pathologically proven frontotemporal dementia presenting with severe amnesia. Brain *128*, 597-605. 10.1093/brain/awh348.

Hampel, S., Chung, P., McKellar, C.E., Hall, D., Looger, L.L., and Simpson, J.H. (2011). Drosophila Brainbow: a recombinase-based fluorescence labeling technique to subdivide neural expression patterns. Nat Methods *8*, 253-259. 10.1038/nmeth.1566.

Harbison, S.T., Serrano Negron, Y.L., Hansen, N.F., and Lobell, A.S. (2017). Selection for long and short sleep duration in Drosophila melanogaster reveals the complex genetic network underlying natural variation in sleep. PLoS Genet *13*, e1007098. 10.1371/journal.pgen.1007098.

Hasegawa, M., Arai, T., Akiyama, H., Nonaka, T., Mori, H., Hashimoto, T., Yamazaki, M., and Oyanagi, K. (2007). TDP-43 is deposited in the Guam parkinsonism-dementia complex brains. Brain *130*, 1386-1394. 10.1093/brain/awm065.

Heisenberg, M. (2003). Mushroom body memoir: from maps to models. Nat Rev Neurosci *4*, 266-275. 10.1038/nrn1074.

Hornberger, M., and Piguet, O. (2012). Episodic memory in frontotemporal dementia: a critical review. Brain *135*, 678-692. 10.1093/brain/aws011.

Isabel, G., Pascual, A., and Preat, T. (2004). Exclusive consolidated memory phases in Drosophila. Science *304*, 1024-1027. 10.1126/science.1094932.

Ito, K., Awano, W., Suzuki, K., Hiromi, Y., and Yamamoto, D. (1997). The Drosophila mushroom body is a quadruple structure of clonal units each of which contains a virtually identical set of neurones and glial cells. Development *124*, 761-771. 10.1242/dev.124.4.761.

Jo, M., Lee, S., Jeon, Y.M., Kim, S., Kwon, Y., and Kim, H.J. (2020). The role of TDP-43 propagation in neurodegenerative diseases: integrating insights from clinical and experimental studies. Exp Mol Med *52*, 1652-1662. 10.1038/s12276-020-00513-7.

Joiner, W.J., Crocker, A., White, B.H., and Sehgal, A. (2006). Sleep in Drosophila is regulated by adult mushroom bodies. Nature *441*, 757-760. 10.1038/nature04811.

Josephs, K.A., Murray, M.E., Whitwell, J.L., Parisi, J.E., Petrucelli, L., Jack, C.R., Petersen, R.C., and Dickson, D.W. (2014a). Staging TDP-43 pathology in Alzheimer's disease. Acta Neuropathol *127*, 441-450. 10.1007/s00401-013-1211-9.

Josephs, K.A., Whitwell, J.L., Weigand, S.D., Murray, M.E., Tosakulwong, N., Liesinger, A.M., Petrucelli, L., Senjem, M.L., Knopman, D.S., Boeve, B.F., et al. (2014b). TDP-43 is a key player in the clinical features associated with Alzheimer's disease. Acta Neuropathol *127*, 811-824. 10.1007/s00401-014-1269-z.

Kabashi, E., Valdmanis, P.N., Dion, P., Spiegelman, D., McConkey, B.J., Vande Velde, C., Bouchard, J.P., Lacomblez, L., Pochigaeva, K., Salachas, F., et al. (2008). TARDBP mutations in individuals with sporadic and familial amyotrophic lateral sclerosis. Nat Genet *40*, 572-574. 10.1038/ng.132.

Kamyshev, N.G., Smirnova, G.P., Kamysheva, E.A., Nikiforov, O.N., Parafenyuk, I.V., and Ponomarenko, V.V. (2002). Plasticity of social behavior in Drosophila. Neurosci Behav Physiol *32*, 401-408. 10.1023/a:1015832328023.

Kansal, K., Mareddy, M., Sloane, K.L., Minc, A.A., Rabins, P.V., McGready, J.B., and Onyike, C.U. (2016). Survival in Frontotemporal Dementia Phenotypes: A Meta-Analysis. Dement Geriatr Cogn Disord *41*, 109-122. 10.1159/000443205.

Kassambara, A. (2020). ggpubr: 'ggplot2' Based Publication Ready Plots.

Kassambara, A., Kosinski, M., and Biecek, P. (2021). survminer: Drawing Survival Curves using 'ggplot2'. R package version 0.4.9.

Khalfallah, Y., Kuta, R., Grasmuck, C., Prat, A., Durham, H.D., and Vande Velde, C. (2018). TDP-43 regulation of stress granule dynamics in neurodegenerative disease-relevant cell types. Sci Rep *8*, 7551. 10.1038/s41598-018-25767-0.

Kunz, T., Kraft, K.F., Technau, G.M., and Urbach, R. (2012). Origin of Drosophila mushroom body neuroblasts and generation of divergent embryonic lineages. Development *139*, 2510-2522. 10.1242/dev.077883.

Langellotti, S., Romano, G., Feiguin, F., Baralle, F.E., and Romano, M. (2018). RhoGAPp190: A potential player in tbph-mediated neurodegeneration in Drosophila. PLoS One *13*, e0195845. 10.1371/journal.pone.0195845.

Lehmkuhl, E.M., Loganathan, S., Alsop, E., Blythe, A.D., Kovalik, T., Mortimore, N.P., Barrameda, D., Kueth, C., Eck, R.J., Siddegowda, B.B., et al. (2021). TDP-43 proteinopathy alters the ribosome association of multiple mRNAs including the glypican Dally-like protein (Dlp)/GPC6. Acta Neuropathol Commun *9*, 52. 10.1186/s40478-021-01148-z.

Lewis, S.A., Negelspach, D.C., Kaladchibachi, S., Cowen, S.L., and Fernandez, F. (2017). Spontaneous alternation: A potential gateway to spatial working memory in Drosophila. Neurobiol Learn Mem *142*, 230-235. 10.1016/j.nlm.2017.05.013.

Li, J., Vitiello, M.V., and Gooneratne, N.S. (2018). Sleep in Normal Aging. Sleep Med Clin *13*, 1-11. 10.1016/j.jsmc.2017.09.001.

Li, Y., Ray, P., Rao, E.J., Shi, C., Guo, W., Chen, X., Woodruff, E.A., 3rd, Fushimi, K., and Wu, J.Y. (2010). A Drosophila model for TDP-43 proteinopathy. Proc Natl Acad Sci U S A *107*, 3169-3174. 10.1073/pnas.0913602107.

Liao, Y., Smyth, G.K., and Shi, W. (2014). featureCounts: an efficient general purpose program for assigning sequence reads to genomic features. Bioinformatics *30*, 923-930. 10.1093/bioinformatics/btt656.

Lien, W.Y., Chen, Y.T., Li, Y.J., Wu, J.K., Huang, K.L., Lin, J.R., Lin, S.C., Hou, C.C., Wang, H.D., Wu, C.L., et al. (2020). Lifespan regulation in alpha/beta posterior neurons of the fly mushroom bodies by Rab27. Aging Cell *19*, e13179. 10.1111/acel.13179.

Ling, J.P., Pletnikova, O., Troncoso, J.C., and Wong, P.C. (2015). TDP-43 repression of nonconserved cryptic exons is compromised in ALS-FTD. Science *349*, 650-655. 10.1126/science.aab0983.

Ling, S.C., Polymenidou, M., and Cleveland, D.W. (2013). Converging mechanisms in ALS and FTD: disrupted RNA and protein homeostasis. Neuron *79*, 416-438. 10.1016/j.neuron.2013.07.033.

Liu, L., Wolf, R., Ernst, R., and Heisenberg, M. (1999). Context generalization in Drosophila visual learning requires the mushroom bodies. Nature *400*, 753-756. 10.1038/23456.

Loganathan, S., Wilson, B.A., Carey, S.B., Manzo, E., Joardar, A., Ugur, B., and Zarnescu, D.C. (2022). TDP-43 Proteinopathy Causes Broad Metabolic Alterations including TCA Cycle Intermediates and Dopamine Levels in Drosophila Models of ALS. Metabolites *12*. 10.3390/metabo12020101.

Loi, S.M., Tsoukra, P., Chen, Z., Wibawa, P., Eratne, D., Kelso, W., Walterfang, M., and Velakoulis, D. (2021). Risk factors to mortality and causes of death in frontotemporal dementia: An Australian perspective. Int J Geriatr Psychiatry *37*. 10.1002/gps.5668.

Love, M.I., Huber, W., and Anders, S. (2014). Moderated estimation of fold change and dispersion for RNA-seq data with DESeq2. Genome Biol *15*, 550. 10.1186/s13059-014-0550-8.

Lu, Y., Ferris, J., and Gao, F.B. (2009). Frontotemporal dementia and amyotrophic lateral sclerosis-associated disease protein TDP-43 promotes dendritic branching. Mol Brain *2*, 30. 10.1186/1756-6606-2-30.

Mackenzie, I.R., Bigio, E.H., Ince, P.G., Geser, F., Neumann, M., Cairns, N.J., Kwong, L.K., Forman, M.S., Ravits, J., Stewart, H., et al. (2007). Pathological TDP-43 distinguishes sporadic amyotrophic lateral sclerosis from amyotrophic lateral sclerosis with SOD1 mutations. Ann Neurol *61*, 427-434. 10.1002/ana.21147.

Mackenzie, I.R., Neumann, M., Baborie, A., Sampathu, D.M., Du Plessis, D., Jaros, E., Perry, R.H., Trojanowski, J.Q., Mann, D.M., and Lee, V.M. (2011). A harmonized classification system for FTLD-TDP pathology. Acta Neuropathol *122*, 111-113. 10.1007/s00401-011-0845-8.

Mackenzie, I.R.A., Rademakers, R., and Neumann, M. (2010). TDP-43 and FUS in amyotrophic lateral sclerosis and frontotemporal dementia. The Lancet Neurology *9*, 995-1007. 10.1016/s1474-4422(10)70195-2.

Manzo, E., Lorenzini, I., Barrameda, D., O'Conner, A.G., Barrows, J.M., Starr, A., Kovalik, T., Rabichow, B.E., Lehmkuhl, E.M., Shreiner, D.D., et al. (2019). Glycolysis upregulation is neuroprotective as a compensatory mechanism in ALS. Elife *8*. 10.7554/eLife.45114.

Mariano, V., Achsel, T., Bagni, C., and Kanellopoulos, A.K. (2020). Modelling Learning and Memory in Drosophila to Understand Intellectual Disabilities. Neuroscience *445*, 12-30. 10.1016/j.neuroscience.2020.07.034.

McAleese, K.E., Walker, L., Erskine, D., Thomas, A.J., McKeith, I.G., and Attems, J. (2017). TDP-43 pathology in Alzheimer's disease, dementia with Lewy bodies and ageing. Brain Pathol *27*, 472-479. 10.1111/bpa.12424.

McCarter, S.J., St Louis, E.K., and Boeve, B.F. (2016). Sleep Disturbances in Frontotemporal Dementia. Curr Neurol Neurosci Rep *16*, 85. 10.1007/s11910-016-0680-3.

McDonald, K.K., Aulas, A., Destroismaisons, L., Pickles, S., Beleac, E., Camu, W., Rouleau, G.A., and Vande Velde, C. (2011). TAR DNA-binding protein 43 (TDP-43) regulates stress granule dynamics via differential regulation of G3BP and TIA-1. Human Molecular Genetics *20*, 1400-1410. 10.1093/hmg/ddr021.

Meneses, A., Koga, S., O'Leary, J., Dickson, D.W., Bu, G., and Zhao, N. (2021). TDP-43 Pathology in Alzheimer's Disease. Mol Neurodegener *16*, 84. 10.1186/s13024-021-00503-x.

Mershin, A., Pavlopoulos, E., Fitch, O., Braden, B.C., Nanopoulos, D.V., and Skoulakis, E.M. (2004). Learning and memory deficits upon TAU accumulation in Drosophila mushroom body neurons. Learn Mem *11*, 277-287. 10.1101/lm.70804.

Morante, J., and Desplan, C. (2008). The color-vision circuit in the medulla of Drosophila. Curr Biol *18*, 553-565. 10.1016/j.cub.2008.02.075.

Muqit, M.M., and Feany, M.B. (2002). Modelling neurodegenerative diseases in Drosophila: a fruitful approach? Nat Rev Neurosci *3*, 237-243. 10.1038/nrn751.

Murley, A.G., and Rowe, J.B. (2018). Neurotransmitter deficits from frontotemporal lobar degeneration. Brain *141*, 1263-1285. 10.1093/brain/awx327.

Murphy, S.L., Kochanek, K.D., Xu, J., and Aria, E. (2021). Mortality in the United States, 2020. U.S. Department of Health and Human Services. https://www.cdc.gov/nchs/data/databriefs/db427.pdf.

Nana, A.L., Sidhu, M., Gaus, S.E., Hwang, J.L., Li, L., Park, Y., Kim, E.J., Pasquini, L., Allen, I.E., Rankin, K.P., et al. (2019). Neurons selectively targeted in frontotemporal dementia reveal early stage TDP-43 pathobiology. Acta Neuropathol *137*, 27-46. 10.1007/s00401-018-1942-8.

Neumann, M., Sampathu, D.M., Kwong, L.K., Truax, A.C., Micsenyi, M.C., Chou, T.T., Bruce, J., Schuck, T., Grossman, M., Clark, C.M., et al. (2006). Ubiquitinated TDP-43 in frontotemporal lobar degeneration and amyotrophic lateral sclerosis. Science *314*, 130-133. 10.1126/science.1134108.

Ostrowski, D., Kahsai, L., Kramer, E.F., Knutson, P., and Zars, T. (2015). Place memory retention in Drosophila. Neurobiol Learn Mem *123*, 217-224. 10.1016/j.nlm.2015.06.015.

Pennington, C., Hodges, J.R., and Hornberger, M. (2011). Neural correlates of episodic memory in behavioral variant frontotemporal dementia. J Alzheimers Dis *24*, 261-268. 10.3233/JAD-2011-101668.

Perry, D.C., Brown, J.A., Possin, K.L., Datta, S., Trujillo, A., Radke, A., Karydas, A., Kornak, J., Sias, A.C., Rabinovici, G.D., et al. (2017). Clinicopathological correlations in behavioural variant frontotemporal dementia. Brain *140*, 3329-3345. 10.1093/brain/awx254.

Polymenidou, M., Lagier-Tourenne, C., Hutt, K.R., Huelga, S.C., Moran, J., Liang, T.Y., Ling, S.-C., Sun, E., Wancewicz, E., Mazur, C., et al. (2011). Long pre-mRNA depletion and RNA missplicing contribute to neuronal vulnerability from loss of TDP-43. Nature Neuroscience *14*, 459-468. 10.1038/nn.2779.

Poos, J.M., Jiskoot, L.C., Papma, J.M., van Swieten, J.C., and van den Berg, E. (2018). Meta-analytic Review of Memory Impairment in Behavioral Variant Frontotemporal Dementia. J Int Neuropsychol Soc *24*, 593-605. 10.1017/S1355617718000115.

Ramaswami, M., Taylor, J.P., and Parker, R. (2013). Altered Ribostasis: RNA-Protein Granules in Degenerative Disorders. Cell *154*, 727-736. 10.1016/j.cell.2013.07.038.

Rascovsky, K., Hodges, J.R., Knopman, D., Mendez, M.F., Kramer, J.H., Neuhaus, J., van Swieten, J.C., Seelaar, H., Dopper, E.G., Onyike, C.U., et al. (2011). Sensitivity of revised diagnostic criteria for the behavioural variant of frontotemporal dementia. Brain *134*, 2456-2477. 10.1093/brain/awr179.

Rawson, J.M., Dimitroff, B., Johnson, K.G., Rawson, J.M., Ge, X., Van Vactor, D., and Selleck, S.B. (2005). The heparan sulfate proteoglycans Dally-like and Syndecan have distinct functions in axon guidance and visual-system assembly in Drosophila. Curr Biol *15*, 833-838. 10.1016/j.cub.2005.03.039.

Rohn, T.T. (2008). Caspase-cleaved TAR DNA-binding protein-43 is a major pathological finding in Alzheimer's disease. Brain Research *1228*, 189-198. 10.1016/j.brainres.2008.06.094.

Romano, M., Feiguin, F., and Buratti, E. (2012). Drosophila Answers to TDP-43 Proteinopathies. J Amino Acids *2012*, 356081. 10.1155/2012/356081.

Rutherford, N.J., Zhang, Y.J., Baker, M., Gass, J.M., Finch, N.A., Xu, Y.F., Stewart, H., Kelley, B.J., Kuntz, K., Crook, R.J., et al. (2008). Novel mutations in TARDBP (TDP-43) in patients with familial amyotrophic lateral sclerosis. PLoS Genet *4*, e1000193. 10.1371/journal.pgen.1000193.

Sani, T.P., Bond, R.L., Marshall, C.R., Hardy, C.J.D., Russell, L.L., Moore, K.M., Slattery, C.F., Paterson, R.W., Woollacott, I.O.C., Wendi, I.P., et al. (2019). Sleep symptoms in syndromes of frontotemporal dementia and Alzheimer's disease: A proof-of-principle behavioural study. eNeurologicalSci *17*, 100212. 10.1016/j.ensci.2019.100212.

Santiago, J.A., Bottero, V., and Potashkin, J.A. (2020). Transcriptomic and Network Analysis Identifies Shared and Unique Pathways across Dementia Spectrum Disorders. Int J Mol Sci *21*. 10.3390/ijms21062050.

Seeley, W.W. (2008). Selective functional, regional, and neuronal vulnerability in frontotemporal dementia. Curr Opin Neurol *21*, 701-707. 10.1097/WCO.0b013e3283168e2d.

Shaw, P.J., Cirelli, C., Greenspan, R.J., and Tononi, G. (2000). Correlates of sleep and waking in Drosophila melanogaster. Science *287*, 1834-1837. 10.1126/science.287.5459.1834.

Sherman, B.T., Hao, M., Qiu, J., Jiao, X., Baseler, M.W., Lane, H.C., Imamichi, T., and Chang, W. (2022). DAVID: a web server for functional enrichment analysis and functional annotation of gene lists (2021 update). Nucleic Acids Res *50*, W216-221. 10.1093/nar/gkac194.

Sreedharan, J., Blair, I.P., Tripathi, V.B., Hu, X., Vance, C., Rogelj, B., Ackerley, S., Durnall, J.C., Williams, K.L., Buratti, E., et al. (2008). TDP-43 Mutations in Familial and Sporadic Amyotrophic Lateral Sclerosis. Science *319*, 1668-1672. 10.1126/science.1154584.

Sreedharan, J., Neukomm, L.J., Brown, R.H., Jr., and Freeman, M.R. (2015). Age-Dependent TDP-43-Mediated Motor Neuron Degeneration Requires GSK3, hat-trick, and xmas-2. Curr Biol *25*, 2130-2136. 10.1016/j.cub.2015.06.045.

Stewart, B.A., Atwood, H.L., Renger, J.J., Wang, J., and Wu, C.F. (1994). Improved stability of Drosophila larval neuromuscular preparations in haemolymph-like physiological solutions. J Comp Physiol A *175*, 179-191. 10.1007/BF00215114.

Stopford, C.L., Thompson, J.C., Neary, D., Richardson, A.M., and Snowden, J.S. (2012). Working memory, attention, and executive function in Alzheimer's disease and frontotemporal dementia. Cortex *48*, 429-446. 10.1016/j.cortex.2010.12.002.

Strausfeld, N.J., and Hirth, F. (2013). Deep homology of arthropod central complex and vertebrate basal ganglia. Science *340*, 157-161. 10.1126/science.1231828.

Sun, Y., Qiu, R., Li, X., Cheng, Y., Gao, S., Kong, F., Liu, L., and Zhu, Y. (2020). Social attraction in Drosophila is regulated by the mushroom body and serotonergic system. Nat Commun *11*, 5350. 10.1038/s41467-020-19102-3.

Susnjar, U., Skrabar, N., Brown, A.L., Abbassi, Y., Phatnani, H., Consortium, N.A., Cortese, A., Cereda, C., Bugiardini, E., Cardani, R., et al. (2022). Cell environment shapes TDP-43 function with implications in neuronal and muscle disease. Commun Biol *5*, 314. 10.1038/s42003-022-03253-8.

Swain, A., Misulovin, Z., Pherson, M., Gause, M., Mihindukulasuriya, K., Rickels, R.A., Shilatifard, A., and Dorsett, D. (2016). Drosophila TDP-43 RNA-Binding Protein Facilitates Association of Sister Chromatid Cohesion Proteins with Genes, Enhancers and Polycomb Response Elements. PLoS Genet *12*, e1006331. 10.1371/journal.pgen.1006331.

Team, R. (2022). RStudio: Integrated Development Environment for R. (PBC).

Team, R.C. (2021). A language and environment for statistical computing. (R Foundation for Statistical Computing).

Therneau, T.M. (2021). _A Package for Survival Analysis in R_. R package version 3.2-13.

Tollervey, J.R., Curk, T., Rogelj, B., Briese, M., Cereda, M., Kayikci, M., König, J., Hortobágyi, T., Nishimura, A.L., Župunski, V., et al. (2011). Characterizing the RNA targets and position-dependent splicing regulation by TDP-43. Nature Neuroscience *14*, 452-458. 10.1038/nn.2778.

Tsao, C.H., Chen, C.C., Lin, C.H., Yang, H.Y., and Lin, S. (2018). Drosophila mushroom bodies integrate hunger and satiety signals to control innate food-seeking behavior. Elife *7*. 10.7554/eLife.35264.

Vogt, K., Schnaitmann, C., Dylla, K.V., Knapek, S., Aso, Y., Rubin, G.M., and Tanimoto, H. (2014). Shared mushroom body circuits underlie visual and olfactory memories in Drosophila. Elife *3*, e02395. 10.7554/eLife.02395.

Waghmare, I., Wang, X., and Page-McCaw, A. (2020). Dally-like protein sequesters multiple Wnt ligands in the Drosophila germarium. Dev Biol *464*, 88-102. 10.1016/j.ydbio.2020.05.004.

Walker, A.K., Spiller, K.J., Ge, G., Zheng, A., Xu, Y., Zhou, M., Tripathy, K., Kwong, L.K., Trojanowski, J.Q., and Lee, V.M.Y. (2015). Functional recovery in new mouse models of

ALS/FTLD after clearance of pathological cytoplasmic TDP-43. Acta Neuropathologica *130*, 643-660. 10.1007/s00401-015-1460-x.

Wickham, H., Averick, M., Bryan, J., Chang, W., McGowan, L., François, R., Grolemund, G., Hayes, A., Henry, L., Hester, J., et al. (2019). Welcome to the Tidyverse. Journal of Open Source Software *4*. 10.21105/joss.01686.

Wolff, G.H., and Strausfeld, N.J. (2016). Genealogical correspondence of a forebrain centre implies an executive brain in the protostome-deuterostome bilaterian ancestor. Philos Trans R Soc Lond B Biol Sci *371*, 20150055. 10.1098/rstb.2015.0055.

Xiao, S., Sanelli, T., Dib, S., Sheps, D., Findlater, J., Bilbao, J., Keith, J., Zinman, L., Rogaeva, E., and Robertson, J. (2011). RNA targets of TDP-43 identified by UV-CLIP are deregulated in ALS. Mol Cell Neurosci *47*, 167-180. 10.1016/j.mcn.2011.02.013.

Yamazaki, D., Horiuchi, J., Nakagami, Y., Nagano, S., Tamura, T., and Saitoe, M. (2007). The Drosophila DCO mutation suppresses age-related memory impairment without affecting lifespan. Nat Neurosci *10*, 478-484. 10.1038/nn1863.

Yan, D., Wu, Y., Feng, Y., Lin, S.C., and Lin, X. (2009). The core protein of glypican Dally-like determines its biphasic activity in wingless morphogen signaling. Dev Cell *17*, 470-481. 10.1016/j.devcel.2009.09.001.

Yu, H.H., and Lee, T. (2007). Neuronal temporal identity in post-embryonic Drosophila brain. Trends Neurosci *30*, 520-526. 10.1016/j.tins.2007.07.003.

Zhan, L., Hanson, K.A., Kim, S.H., Tare, A., and Tibbetts, R.S. (2013). Identification of genetic modifiers of TDP-43 neurotoxicity in Drosophila. PLoS One *8*, e57214. 10.1371/journal.pone.0057214.

Zhang, K., Guo, J.Z., Peng, Y., Xi, W., and Guo, A. (2007). Dopamine-mushroom body circuit regulates saliency-based decision-making in Drosophila. Science *316*, 1901-1904. 10.1126/science.1137357.

Zwarts, L., Vanden Broeck, L., Cappuyns, E., Ayroles, J.F., Magwire, M.M., Vulsteke, V., Clements, J., Mackay, T.F., and Callaerts, P. (2015). The genetic basis of natural variation in mushroom body size in Drosophila melanogaster. Nat Commun *6*, 10115. 10.1038/ncomms10115.